ADDIS ABABA UNIVERSITY
SCHOOL OF GRADUATE STUDIES
DEPARTMENT OF CHEMISTRY

Electrocatalytic Reduction of Molecular Oxygen at Poly (1, 8-Diaminonaphthalene) and Polypyrrole Multi-Wall Carbon Nanotubes Modified Glassy Carbon Electrodes

By

Kibret Melaku

Advisor: Dr. Shimelis Admassie

June, 2010

Electrocatalytic Reduction of Molecular Oxygen at Poly (1, 8-Diaminonaphthalene) and Polypyrrole Multi-Wall Carbon Nanotubes Modified Glassy Carbon Electrodes

A Graduate Project (Chem. 774) Submitted to the School of Graduate Studies, Addis Ababa University

By

Kibret Melaku

Advisor: Dr. Shimelis Admassie

June, 2010

Table of Contents

ACKNOWLEDGEMENTS

It is a great pleasure to acknowledge my advisor, Dr. Shimelis Admassie for his continuous guidance, encouragement, creating conducive environment and support with materials during the course of the project.

List of Figures

List of Tables

LIST OF ABBREVIATIONS

CNTs ……. carbon nanotubes

CP ……. conducting polymers

CV ……. cyclic Voltammetry

1, 8-DAN ……. 1, 8- Diaminonaphthalene

ECM ……. electrochemical modification

EGCG ……. Epigallocatechin gallate

E_{pa} ……. Peak potential

GC ……. glassy carbon electrode

I_{pa} ……. Peak current

K- L ……. Koutecky-Lecich plot

MWCNTs ……. multi wall carbon nanotubes

ORR ……. Oxygen reduction Reaction

PANI ……. polyaniline

PBS ……. PhosphateBuffer Solution

PDDA …….poly (diallyldimethylammonium chloride)

PNR……. poly(neutral red)

PPY ……. Polypyrrole

RDE ……. rotating disk electrode

RDV ……. rotating disk voltammetry

RRDE ……. rotating ring disk electrode

SWCNTs …… single wall carbon nanotubes

Abstract

The electrochemical growth current of poly (1, 8- Diaminonaphthalene) and polypyrrole and their redox currents were enhanced several-fold when deposited on carbon nanotubes modified glassy carbon electrode compared the bare glassy carbon electrode surface. Cyclic voltammetry were used to characterize the modified film on the electrode surface. The electrocatalytic ability of the modified electrodes for the reduction of molecular oxygen was investigated using cyclic voltammetry and rotating disk techniques in 0.2 M $NaSO_4$ (pH=1) solution. GC/MWCNT/p-DAN modified electrode showed good electrocatalytic activity for oxygen reduction reaction. The oxygen reduction behavior of GC/MWCNT/p-DAN electrode at different deposition cycle (5 and 8) of p-DAN was investigated using rotating disk electrodes and compared with each other. The RDE data indicated that the reduction of oxygen on both electrodes of GC/MWCNT/p-DAN proceeds by four-electron pathway in 0.2 M $NaSO_4$ (pH=1) solution. From Koutecky-Levich analysis, the kinetics parameters (total number of exchanged electrons, limiting current, rate constant, exchange current, Tafel slope and transfer coefficient) were determined.

Keywords; Electrocatalysis, Electropolymerization, Multi-walled carbon nanotubes, Oxygen Reduction, poly (1, 8- Diaminonaphthalene), polypyrrole

1. Introduction

Studies on molecular oxygen reduction reaction (ORR) have attracted much attention in modern electrochemistry due to its technological importance in electrochemical devices such as fuel cells, secondary metal-air batteries, corrosion and several industrial processes (table1). In the past several decades it has been studied on various catalytic electrodes in acidic and basic medium. Nobel metals such as platinum, gold, ruthenium, palladium and mixed metals alloys have played a dominating role as electrocatalyst for the ORR. However, the high cost of these metals and sluggish kinetics of ORR restricts the commercial utility as catalyst. A search for the low-cost electrocatalyst for ORR has now been an important goal for many researchers [1, 2].

Explorations of alternative new catalytic materials instead of the noble metals were carried out. These electrocatalyst includes non-noble transition metals and alloys, transition metal macrocyclic compounds, transition metal chalcogenides, carbon materials. Many of these investigations have involved the collection of current – potential data in order to discuss the kinetics and mechanism for ORR in acidic and basic solutions to reveal the intrinsic activities of these materials for the reduction as well as to elucidate the possible reaction pathways [3 - 5].

Dispersion of catalyst materials in a convenient electron conducting substrate is known to enhance the catalytic activity of the electrode [4]. An electrochemically conducting polymer film serves as a conductive matrix for the electron transfer reaction. Composite materials based on the combination of a conducting polymer and carbon nanotube have shown properties of the individual components with synergetic effect [6]. Composite based electrocatalyst for reduction of oxygen is considered as alternative new materials and carried out in this paper.

Table1. Oxygen reduction in electrochemical technology and processes.

Technology/process	System/electrolyte	Electrochemical role
Cathodic reduction of oxygen		
Fuel cells	Alkaline Molten carbonate Phosphoric acid Polymer electrolyte Solid oxide	Cathodic reactant
Metal/air batteries	Al/air Fe/air Li/air Zn/air	Cathode reactant during discharge
H_2O_2 production	Alkaline electrolyte	Cathode reactant
Chlor-alkali production	Air cathode in chlor-alkali cells	Depolarizer reduces energy consumption
Corrosion	Metals, alloys	Depolarizer enhances corrosion rate

This chapter is presented briefly some fundamental concepts of the oxygen reduction reactions, some kinetics and mechanistic aspect of the oxygen reduction reaction and some electrocatalyst designed for electrocatalytic reduction of oxygen.

1.1 General Scheme of Oxygen Reduction

The mechanisms of the electrochemical oxygen reduction reaction have been studied by different researchers. They forwarded mechanism catalyzed by different catalyst in acidic and alkaline solution. Oxygen reduction is a multielectron reaction that usually includes several elementary steps in reaction mechanisms. In aqueous solutions, oxygen reduction reaction appears to occur by two overall pathways; a ‘’direct ‘’ four electron reduction and a ‘’peroxide’’ pathway, which involves H_2O_2 as intermediate [7].

The direct four electron pathway is

$$O_2 + 4H^+ + 4e^- \longrightarrow 2H_2O \qquad E^0 = 1.229 \text{ (in acidic midia)}$$

$$O_2 + H_2O + 4e^- \longrightarrow 4OH^- \qquad E^0 = 0.401 \text{ (in alakaline midia)}$$

The peroxide pathway is

$$O_2 + H_2O + 2e^- \longrightarrow H_2O_2 \quad ; E^0 = 0.67\ V$$

Peroxide can undergo further reduction or decomposition in acid solution, via the reactions

$$H_2O_2 + 2H^+ + 2e^- \longrightarrow 2H_2O \ ; \ E^0 = 1.77\ V$$

or by disproportionation reaction

$$2H_2O_2 \longrightarrow 2H_2O + O_2$$

In alkaline solutions, the reaction

$$O_2 + H_2O + 2e^- \longrightarrow HO^-_2 + OH^- \quad ; E^0 = -0.065V$$

is followed either by further two-electron reduction or by decomposition;

$$HO^-_2 + H_2O + 2e^- \longrightarrow 3OH^- \ ; \ E^0 = 0.867\ V$$

$$2HO^-_2 \longrightarrow 2OH^- + O_2$$

where E° is the standard electrode potential and all potentials refer to the standard state values *vs*. the normal hydrogen electrode at 25 ºC.

The reduction pathways such as the 1-, 2-, and 4- electron reduction pathways have unique significance, depending on the applications. In fuel cell processes, the 4-electron direct pathway is highly preferred. The 2- electron reduction pathway is used in industry for H_2O_2 production. The 1 – electron reduction pathway is of importance in the exploration of the ORR mechanism [8, 9].

Despite the apparent simplicity, these overall reactions represent a complex electrocatalytic network and involve many elementary steps. The dominating pathway depends on several factors, for example, on the electrode material, solution pH and on electrode potential [9].

The principal tool for quantitative determination of the extent of these reactions is the rotating ring –disk technique. Peroxide is the final reduction product on some less active surfaces that support a two-electron reduction. On some surfaces, the two pathways can occur in parallel. When peroxide is not desorbed from the surface before its reduction, it cannot be detected at the ring electrode, and a direct four-electron pathway and a series four- electron pathway are indistinguishable by the existing techniques [5].

The molecular orbital diagram of oxygen molecule is shown in Figure 1 . According to Hund's rule, in the ground-state, O_2 possesses two unpaired electrons located in a doubly degenerate π* antibonding orbital. This corresponds to a triplet state. The bonding orbitals of oxygen molecule can be ascribed to the 3σg orbital with two electrons, the doubly degenerate 1πu and 1πg* orbitals, where the 1πu orbital has double occupancy while the 1πg* orbital has single occupancy. The resulting bond order is two. When O_2 undergoes reduction, the electrons added occupy anti-bonding orbitals, decreasing the bond order of O-O. This increases the O-O bond distance and the vibrational frequency decreases. The excess of bonding over non-bonding electrons in the diagram of Figure 1 is four. This explains the high stability of the O_2 molecule and its relatively low reactivity, in spite of its high oxidizing power [10].

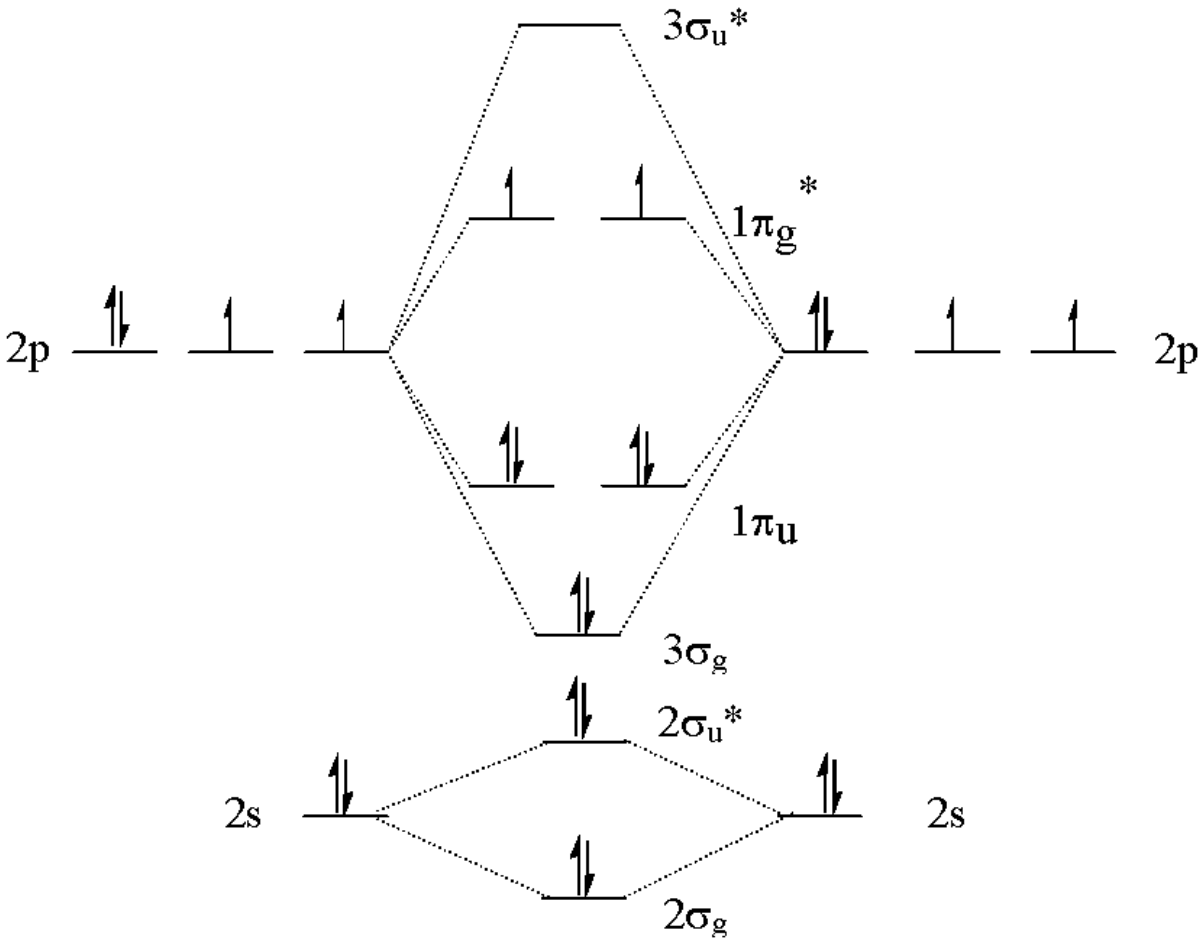

Figure 1. Molecular Orbital diagram of oxygen molecule.

The type of dioxygen interaction with electrode surfaces has been a long –standing question of oxygen electrocatalysis. There is no reliable information on the sites and configuration for oxygen adsorbed on an electrode surface. Oxygen adsorption is a complex process where physiorption, dissociative atomic chemisorptions and oxide formation are all possible. Yeager consider three plausible models for molecular oxygen adsorbed on metal surface shown in Figure 2 [10].

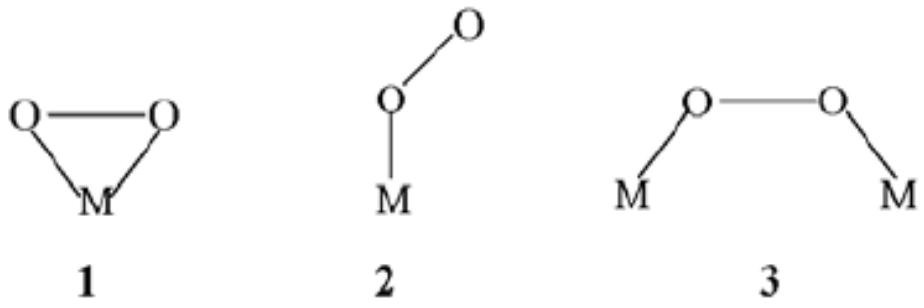

Figure 2**.** Possible configurations of oxygen interaction with a metal in a complex ((1) Griffiths, (2) Pauling models and (3) Bridge (Yeager) models).

i. O_2 interacting with two bonds with a single substrate atom (Griffith model) by forming a bond mainly between its σ orbitals and empty d_z^2 orbitals of the metal surface atom, and by forming a σ back bond from the partially filled d_{xy} and d_{yz} metal orbitals to antibonding π^* orbitals of O_2.
ii. End – on adsorption through a single bond (Pauling model), in a σ- type bond in which a σ orbital of O_2 donates electron density to an acceptor d_z^2 orbital of the metal forming an adsorbed superoxide. This can then accept a second electron to form hydrogen peroxide.
iii. A bridge model, with two bonds with two sites, which was proposed by Yeager principally for the reaction on platinum group metals. Bond breaking then leading to a four- electron transfer process to give water as the final product.

Depending on the mode of adsorption of oxygen molecule on metal surface, different mechanistic steps will occur. The ORR pathways in both acidic and alkaline medium are given below [11].

In case of Bridge interaction, the mechanism of ORR in acidic medium is

$$O_2 + 2e^- + 2H^+ \longrightarrow 2OH_{ads}$$

$$2OH_{ads} + 2H^+ + 2e^- \rightarrow 2H_2O$$

The overall direct reaction;

$$O_2 + 4H^+ + 4e^- \longrightarrow 2H_2O \qquad E^0 = 1.229 \text{ (in acidic midia)}$$

In basic medium,

$$O_2 + 2e^- + 2H_2O \rightarrow 2OH_{ads} + 2OH^-$$

$$2OH_{ads} + 2e^- \rightarrow 2OH^-$$

The overall reaction

$$O_2 + H_2O + 4e^- \longrightarrow 4OH^- \qquad E^0 = 0.401 \text{ (in alakaline midia)}$$

In the case of end -on interaction, the mechanism of ORR in acidic medium is

$$O_2 + e^- + H^+ \longrightarrow HO_{2\,(ads)}$$

$$HO_{2\,(ads)} + e^- + H^+ \longrightarrow H_2O_2$$

The overall indirect reaction

$$O_2 + 2H^+ + 2e^- \longrightarrow H_2O_2$$

$$H_2O_2 + 2H^+ + 2e^- \longrightarrow 2H_2O$$

In basic medium

$$O_2 + H_2O + e^- \longrightarrow HO_{2(ads)} + OH^-$$

$$HO_{2(ads)} + e^- \longrightarrow HO_2^-$$

Overall indirect reaction;

$$O_2 + H_2O + 2e^- \longrightarrow HO_2^- + OH^-$$

1.3 Electrocatalysts for Oxygen Reduction

The essential criteria for a better oxygen reduction electrocatalysts are; high electronic conductivity, chemical and structural stability under the condition namely; operating temperature, wide range of oxygen partial pressure and concentration of electrolyte, ability to decompose the intermediate species formed during the reduction process, tolerant to contaminants and low cost [10].

Oxygen reduction takes place at high positive potentials. At such potentials most of the metals will dissolve and give rise to a similar situation to that prevailing at the cathode i.e., only noble metals and some of their alloys offer possibilities among metallic systems. The

most familiar oxygen reduction catalysts are based on noble metals, particularly platinum. These have been investigated extensively as pure metals, as nanoparticles, and alloys , and as polycrystalline and single crystal surfaces . They show a wide variety of behaviour, reflecting both the surface structure and the presence or absence of oxide films [12].

The widely used catalyst, Pt, suffers from several drawbacks, namely slow kinetics, low efficiency, high cost, and limited abundance in the earth's crust. There has been significant activity in recent years in electrochemistry of oxygen reduction to develop new and low-cost, non-noble metal-based electrocatalysts.

Several different approaches have been examined to substitute Pt and to improve Pt catalyst. These include

(a) modification of the Pt material by alloying,

(b) modification of Pt or related precious metals by decoration of nanoparticles,

(c) use of bioinspired catalysts,

(d) use of graphite and carbon materials,

(e) use of transition metal based catalyst supported on graphite surfaces and

(f) use of transition metal complexes

Among these approaches, transition-metal complexes have been widely investigated for the electrocatalysis of O_2 reduction. Besides these, some reports have been mentioned to the electrocatalysis of O_2 reduction with various chemicals and composite, including polymer, polymer-metals composite, and others [12-14].

2. Carbon Nanotube Composites

2.1 Carbon Nanotubes (CNTs)

Carbon nanotubes have recently attracted considerable interest as a material with extensive potential in various applications based on their remarkable mechanical, electrical properties, good chemical stabilities, and high surface area [15].

CNTs are as the name suggests tubes made of carbon atoms. Elemental carbon in the sp^2 hybridization can form a variety of amazing structures. Apart from the well-known graphite, carbon can build closed and open cages with honeycomb atomic arrangement. The first such structure to be discovered was the C_{60} molecule. Although various carbon cages were studied, in 1991 Iijima observed for the first time tubular carbon structures [16].

Carbon nanotubes are large macromolecules that are unique for their size, shape, and remarkable physical properties like excellent electronic properties, good chemical stability, and large surface areas. They can be thought of as a sheet of graphite (a hexagonal lattice of carbon) rolled into a cylinder. Currently, the physical properties are still being discovered and disputed. What makes it so difficult is that nanotubes have a very broad range of electonic, thermal, and structural properties that change depending on the different kinds of nanotube (defined by its diameter, length, and chirality) [15, 16].

There are two main types of nanotubes available today (Figure 3). Single walled nanotubes (SWNT) consist of a single sheet of graphene rolled seamlessly to form a cylinder with diameter of order of 1- 2 nm and length of up to 0.2 -5 μM. Multi-walled nanotubes (MWNT) consist of an array of such cylinders formed concentrically and separated by 0.36 nm, similar to the basal plane separation in graphite. MWNTs can have diameters from 2 to 25 nm and lengths of tens of microns [16, 17].

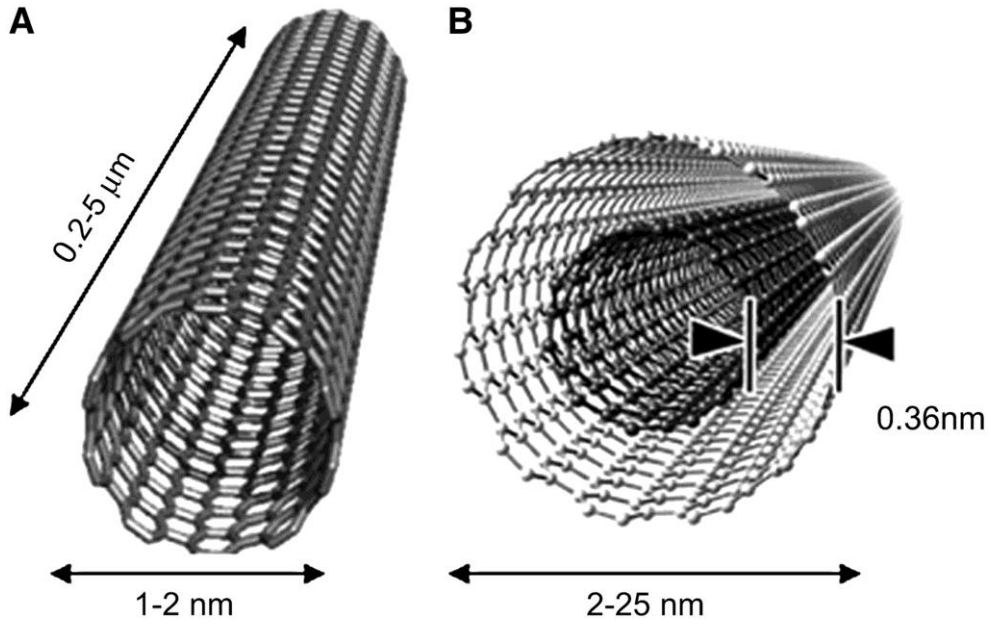

Figure 3: (A) Single wall and (B) multi wall carbon nanotubes

2.1.1Functionalisation of Carbon Nanotubes [18]

Carbon nanotubes consisting of large aggregates, as manufactured, different efforts have been made to disperse to individual fibers by the use of surfactants, sonication and chemical functionalization.The chemical functionalization of CNTs is the formation of new chemical bonds between outside functional groups and some part of the nanotube. The caps of CNTs can be removed and the open ends can be functionalized. Chemical modification of activated carbons nanotubes has been studied in detail. Several methods for attachment of oxygen-containing groups to the CNT surfaces have been developed [17, 19].

Currently, different approaches are reported to improve the dispersion of CNTs in solvents or polymers in order to fabricate the composite mixed matrix nanotubes membrane. Recent reports on the chemical compatibility and dissolution properties of CNTs have promoted a great deal of interests in developing modification and functionalization of their surface [19, 20].

The following section will summarize some of the method used for functionalized carbon nanotubes by different researcher groups.

i. Thermally Activated Chemical Functionalization

The most common and facile method for the surface functionalization of CNTs is nanotube oxidation using acids by heating, which results in the formation of a number of carboxylic acid groups (-COOH), hydroxyl groups (-OH) on the surface of the nanotubes. These functionalized nanotubes are much more stable in polar solvents.

The oxidatively introduced carboxyl groups represent useful sites for further modifications, as they enable the covalent coupling of molecules through the creation of amide and ester bonds. By this method the nanotubes can be provided with a wide range of functional moieties, for which purpose bifunctional molecules (e.g., diamines) are often utilized as linkers.

The presence of (modified) carboxyl groups leads to a reduction of van der Waals interactions between the CNTs, which strongly facilitates the separation of nanotube bundles into individual tubes. Additionally, the attachment of suitable groups renders the tubes soluble in aqueous or organic solvents, opening the possibility of further modifications through subsequent solution-based chemistry.
While the two-step functionalization of nanotubes through the oxidative introduction of carboxyl groups followed by the formation of amide or ester linkages does allow for a stable chemical modification, it has only a relatively weak influence on the electrical and mechanical properties of the nanotubes.

ii. Electrochemical Modification of Nanotubes

Electrochemistry has been developed into an elegant tool for the functionalization of CNTs in a selective and controlled manner. A constant potential (potentiostatic) or a constant current (galvanostatic) is applied to a CNT electrode immersed in a solution that contains a suitable reagent, whereby a highly reactive (radical) species is generated through electron transfer between the CNT and the reagent. Many organic radical species have a tendency to react with the starting reagent or to self-polymerize, resulting in a polymer coating on the tubes.
Depending on the reagent used, the polymeric layer may or may not be bonded in a covalent manner on to the nanotube sidewall. In addition to being simple, clean, and efficient, electrochemical modification (ECM) schemes are quite versatile in that they allow for an

accurate control over the extent of film deposition through the choice of suitable electrochemical conditions, that is, the duration and magnitude of the applied potential. For example, via electrochemical coupling of aromatic diazonium salts, phenyl residues have been covalently grafted onto bulk samples of SWCNTs. The coupling mechanism has been interpreted to involve the transfer of an electron from the CNT, which reduces the diazonium salt to a highly reactive phenyl radical and then attaches covalently to the sidewall.

iii. Photochemical Functionalization of Nanotubes

In contrast to the chemical functionalization routes based upon thermally activated chemistry or electrochemistry, photochemical approaches have been employed to a much lesser extent up to now. Photoirradiation has been used to generate reactive species such as nitrenes in the course of sidewall addition reactions.

Carbon radicals are highly reactive species and can be in general generated in three different ways: photo-chemically, thermally and in oxidation–reduction reactions. As the precursor compound, from which thermally generated radicals, organic peroxides were used.These organic peroxides thermally decompose to carbon radicals and CO_2. This is an advantage for the large-scale functionalization of CNTs because the only by-product is CO_2. Once the reaction is finished there is no need for extra separation of either side products or non-reacted species from the reaction mixture.

2.2 Conducting Polymer [21]

The high application potential of conducting polymers (CP) in chemical and biological sensors is one of the main reasons for the intensive investigation and development of these materials. Most CP were synthesized by modification of the structures shown in Figure 4.

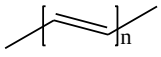

polyacetylene

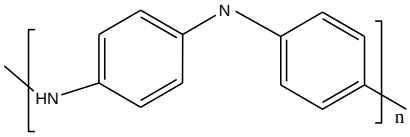

polyaniline

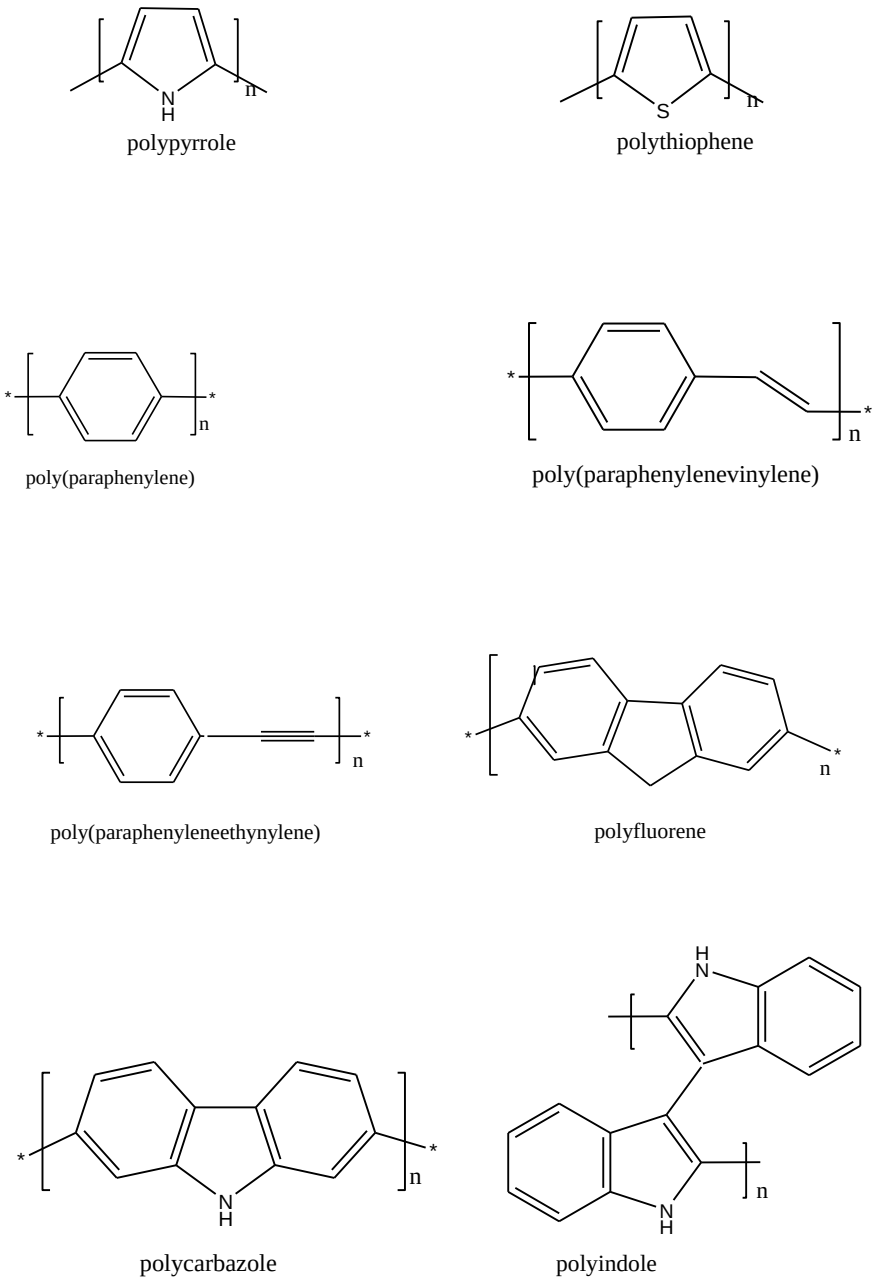

Figure 4- Main classes of conductive polymers.

CP show almost no conductivity in the neutral (uncharged) state. Their intrinsic conductivity results from the formation of charge carriers upon oxidizing (*p*-doping) or reducing (*n*-doping) their conjugated backbone. Oxidation of the neutral polymer and following relaxation processes causes the generation of localized electronic states and a so-called polaron is formed. If now an additional electron is removed, it is energetically more

favourable to remove the second electron from the polaron than from another part of the polymer chain. This leads to the formation of one bipolaron rather than two polarons. However it is important to note that before bipolaron formation the entire CP chain would first become saturated with polarons.

Doping of CP can be done either chemically or electrochemically. Chemical doping is effective but poor reproducible quantitatively. Alternatively, electrochemical doping provides fine tuning of the doping level by adjusting the electrical potential. The unique properties of conducting polymers are used in various chemical and biological sensors, electrocatalyst and catalyst matrix.

2.3 Carbon Nanotubes Composites

The preparation of composite materials, based on integration of CNTs with some other materials possessing well-known electrochemical significance, has led to the achievement of modified electrode surfaces that exhibit special properties due to the synergic effect from the individual components. Materials used for such purposes mostly include polymers and metal nanoparticles.[22]

The effective use of CNTs in composite applications depends on the ability to disperse the CNTs uniformly throughout the matrix without reducing their aspect ratio. Due to the van der Waals attraction, nanotubes are held together as bundles and ropes. Thus they have very low solubility in solvents and tend to remain as entangled agglomerates. To overcome the difficulty of dispersion, mechanical/physical methods such as ultrasonication, surfactant addition, melt blending and chemical modification through functionalization were used [22].

To date, a large variety of possible composite materials using SWCNTs and MWCNTs combined either with different polymers or with inorganic compounds has been prepared. Composites with inorganic metal matrix reinforced with CNTs are expected to have unique mechanical properties. Using CNTs as reinforcing additive, either in metal- or polymer-based composites are prepared [22].

2.3. 1 Carbon Nanotubes-Conducting Polymer Composites

When considering MWCNT/ polymer composites in general, it was found that there was an increase in electrical conductivity of the composite compared to the pristine polymer of nearly eight orders of magnitude [23].

There has been intense recent research concerning the fabrication, characterization and application of polymer– carbon nanotube composites, driven by a growing recognition of the unique mechanical, electrical, thermal and other materials-related properties of carbon nanotubes. Presently, the chemical functionalization and solubilization of carbon nanotubes has emerged as an effective means for the homogeneous dispersion of carbon nanotubes in solution and for the subsequent wet-casting of polymer–carbon nanocomposite films [24].

The properties of polymer nanocomposites containing carbon nanotubes depend on several factors in addition to the polymer: synthetic process used to produce nanotubes; nanotube purification process (if any); amount and type of impurities in the nanotubes; diameter, length, and aspect ratio of the nanotubes objects in the composite (isolated, ropes, and/or bundles); nanotubes orientation in the polymer matrix [16].

The main obstacles to overcome in the research of CNT-based composite materials are (i) the wettability of the CNT surface, (ii) the load transfer from the matrix to the nanotubes and (iii) the ability to disperse CNTs homogeneously into the matrix. One possible way to achieve these requirements is chemical functionalization; the interaction between nanotubes and the matrix can be significantly improved when chemically functionalized CNTs are employed instead of pristine CNTs [24].

Some composite based on CNTs and conducting polymer have been prepared for application in chemical sensor, electrocatalyst, capacitor, and for different purpose [25]. Composite of high molecular weight polyanaline and carbon nanotubes were prepared using different ways of functionalizing of nanotubes. A microwave-assisted hydrothermal digestion process was employed to functionalize MWCNTs in a diluted HNO_3 solution in a closed vessel. This approach used to obtain acidic suspensions of MWCNTs with good dispersion stability, in which alkaline aniline monomers could be dissolved. The resulting mixture was then used directly to grow *in situ* MWCNT/PANI composite coatings of various thicknesses, up to a

couple of millimeters, onto graphite electrodes by galvanostatic polymerization. The as-grown composite coatings were investigated in detail for electrochemical capacitor applications [26].

K.M. Manesh etal prepare the composite by amine functionalization of MWCNT with poly (ethylene glycol) bis (3- aminopropyl). The polymer film, PANI-g-MWCNT, was deposited by electrochemical grafting of PANI onto functionalized MWCNT. GC/PANI/-g-MWCNT modified electrode used as electrocatalyst for oxygen reduction reaction [27]. Amine functionalized MWCNT was used also to graft polydiphenylamine (PDPA) on ITO electrode using cyclic voltammetry deposition. This modified electrode has pronounced electrocatalytic behavior towards the reduction of H_2O_2 with a linear dependence in current response with the concentration of H_2O_2 [28].

Yogeswaran et al. have developed a novel composite material with the functionalized MWCNTs with poly(neutral red) (f-MWCNTs-PNR) at the GCE, gold, and ITO electrode surface using PBS and H_2SO_4 for pH 6.0 and 1.0, respectively. The preparation of the composite electrodes involves, converting the hydrophobic nature of the MWCNTs into a hydrophilic nature by means of functionalization. Then, the bare electrode has been modified and the PNR is electropolymerized from an aqueous solution. The f-MWCNTs-PNR composite films have a good catalytic activity on biochemical compounds such as EGCG, NADH, epinephrine, and serotonin. A detailed study was conducted to elucidate the role of f-MWCNTs with PNR, its effect on catalytic activity such as changes in Epa and Ipa.[29]

Nanotube/Polymer Composites prepared using different methods, the most commonly used methods are; [30]

Solution Blending. This is the most common method for fabricating polymer nanocomposites because it is both amenable to small sample sizes and effective. Solution blending involves three major steps: disperse nanotubes in a suitable solvent, mix with the polymer (at room temperature or elevated temperature), and recover the composite by precipitating or casting a film.

Melt Blending. Melt blending uses high temperature and high shear forces to disperse nanotubes in a polymer matrix and is most compatible with current industrial practices. However, relative to solution blending methods, melt blending is generally less effective at dispersing nanotubes in polymers and is limited to lower concentrations due to the high viscosities of the composites at higher nanotube loadings.

In Situ Polymerization. This fabrication strategy starts by dispersing nanotubes in monomer followed by polymerizing the monomers. As with solution blending, functionalized nanotubes can improve the initial dispersion of the nanotubes in the liquid (monomer, solvent) and consequently in the composites. Furthermore, in situ polymerization methods enable covalent bonding between functionalized nanotubes and the polymer matrix using various condensation reactions.

2.3.2. Carbon Nanotubes–Nanoparticles Composites

For a long time, active carbon has found widespread application as a support material in heterogeneous catalysis. Compared to this form of carbon, carbon nanotubes offer the advantage of a more defined morphology and chemical composition as well as the possibility to attach catalysts onto their surface [31].

Metal nanaoparticles- carbon nanotube composites are important because novel catalysts can be developed. Incorporation of nanoparticles to CNTs for the modification of electrodes has been demonstrated to enhance the electrocatalytic activity of many electrochemical processes [32-34].

Electrochemistry provides a simple but efficient route for the decoration of nanotubes with metal nanoparticles. In such an experiment, a metal salt in solution is reduced by application of an appropriate potential. Electrodeposition offers several advantages over alternative methods such as metal evaporation or deposition of pre-formed colloid particles, most importantly good control over the size and density of the particles. In addition, electrochemically decorated particles are in intimate contact with the carbon nanotubes in comparison to metal colloids deposited from solution, which is important for some applications. CNTs decorated with transition metals like platinum or palladium are interesting as catalysts with high surface area or as chemical sensors [24, 32, 33].
Compton and co-workers have recently reviewed the methods used for the preparation of CNT supported metal nanoparticles and their further applications [35]. As has been recently published, different metal nanoparticles (Pt, Cu, Pd,Au) can be attached to the surface of carbon nanotubes and these hybrid electrodes demonstrate a high electrocatalytic activity towards various bioelectrochemical reactions [31]. Xiang-Rong Ye et.al, prepare the multiwall carbon nanotubes composite of nanoparticles (palladium, rhodium and ruthenium)

by deposited onto functionalized MWCNTs through a simple hydrogen reduction of metal β –diketone precursors in supercritical carbon dioxide. The Pd/MWCNT composite shows high electrocatalytic activities in ORR and hydrogenation of olefins in carbon dioxide [24] Yang et.al prepare Ag/CNTs by deposition of Ag nanoparticles on carbon nanotubes as a catalyst for hydrazine oxidation [32].

2.4 Electrocatalyst for Oxygen Reduction based on Carbon Nanotubes Composite

Metal nanoparticles have received considerable attention in recent years. Incorporation of nanoparticles to CNTs for the modification of electrodes has been demonstrated to enhance the electrocatalytic activity of many electrochemical processes. The composite of carbon nanotubes and gold nanoparticles were used to fabricate modified GC electrodes for electrocatalytic reduction of oxygen in 0.5 M H_2SO_4 solution. The kinetic parameters of oxygen reduction were determined and the specific activity of the composite electrode was slightly higher than that of the bulk Au electrode [36].

The multi-walled carbon nanotubes (MWNTs) modified glassy carbon electrode exhibited electrocatalytic activity to the reduction of oxygen in 0.1 acetate (pH 3.8) buffer solution. Further modification with cobalt porphyrin film on the MWNTs by adsorption, the resulted modified electrode showed more efficient catalytic activity to O_2 reduction. The reduction potential shifted to the positive direction and the reduction current increased significantly at the modified electrode [37].

The composite film of polyaniline (PANI) and multi-wall carbon nanotube was prepared on the surface of glassy carbon electrode by electropolymerization of a mixture of amine functionalized MWCNT and aniline. The electrocatalytic activity for ORR was demonstrated using cyclic voltammetry and exhibits remarkable electrocatalytic activity [38].

The gold nanoparticles, poly (diallyldimethylammonium chloride) (PDDA) and MWCNT composite was prepared by immersing the cleaned GC electrode into MWCNT- PDDA suspension at room temperature. Afterwards the electrode was immersed in Au nanoparticles solution. The oxygen reduction behaviour of the AuNP/PDDA-MWCNT modified GC electrodes was studied using CV methods and the catalysts showed a remarkable electrocatalytic activity towards O_2 reduction in acid media [35].

3. Theoretical Backgrounds

3. 1 Electrode Process

Electrode process involves all the changes and processes occurring at the electrode or in its vicinity while current flows through the cell. Electrode processes consist of the electrode reaction and the mass transport process [39].

One kind comprises reactions in which charges (e.g., electrons) are transferred across the metal-solution interface. Electron transfer causes oxidation or reduction to occur. Since such reactions are governed by Faraday's law (i.e., the amount of chemical reaction caused by the flow of current is proportional to the amount of electricity passed), they are called faradaic processes. Electrodes at which faradaic processes occur are sometimes called charge transfer electrodes. However, processes such as adsorption and desorption can occur, and the structure of the electrode-solution interface can change with changing potential or solution composition. These processes are called nonfaradaic processes. Both faradaic and nonfaradaic processes occur when electrode reactions take place [39, 40].

The pathways of the electrode reaction can be quite complicated, and takes place in a sequence that involves several steps. The rate of such reactions is determined by the slowest step in the sequence. Simple reactions involve only mass transport of the electroactive species to the electrode surface, the electron transfer across the interface, and the transport of the product back to the bulk solution. More complex reactions include additional chemical and surface processes that precede or follow the actual electron transfer. The net rate of the reaction, and hence the measured current, may be limited either by mass transport of the reactant or by the rate of electron transfer. The more sluggish process will be the rate-determining step. Whether a given reaction is controlled by the mass transport or electron transfer is usually determined by the type of compound bening measured and by various experimental conditions (electrode material, media, operating potential, mode of mass transport, time scale, etc.). For a given system, the rate-determining step may thus depend on the potential range under investigation. When the overall reaction is controlled solely by the rate at which the electroactive species reach the surface (i.e., a facile electron transfer), the current is said to be mass transport-limited. Such reactions are called nernstian or reversible, because they obey thermodynamic relationships. Several important techniques rely on such mass transport-limited conditions [39, 40].

Mass transfer, that is, the movement of material from one location in solution to another, arises either from differences in electrical or chemical potential at the two locations or from movement of a volume element of solution. The modes of mass transfer are:

1. *Migration.* Movement of a charged body under the influence of an electric field (a gradient of electrical potential).
2. *Diffusion.* Movement of a species under the influence of a gradient of chemical potential (i.e., a concentration gradient).
3. *Convection.* Stirring or hydrodynamic transport. Generally fluid flow occurs because of *natural convection* (convection caused by density gradients) and *forced convection,* and may be characterized by stagnant regions, laminar flow, and turbulent flow.

3.2 Techniques used in Electrocatalytic ORR

The most frequently used techniques for ORR catalysis studies are steady-state polarization, cyclic voltammetry, rotating disk electrode (RDE), and rotating ring disk electrode (RRDE).

3.2.1 Steady state polarization [39]

Information about an electrode reaction is often gained by determining current as a function of potential (by obtaining *i-E* curves). Certain terms are sometimes associated with features of the curves. If a cell has a defined equilibrium potential, that potential is an important reference point of the system. The departure of the electrode potential (or cell potential) from the equilibrium value upon passage of faradaic current is termed polarization. The extent of polarization is measured by the overpotential, η,

$$\eta = E^o - E \qquad 1$$

Current-potential curves, particularly those obtained under steady-state conditions, are sometimes called polarization curves. In general, for an elementary electrochemical reaction, O + e- = R, the polarization follows the Butler-Volmer equation:

$$i = i^o\left(e^{-\frac{\alpha F\eta}{RT}} - e^{\frac{(1-\alpha)F\eta}{RT}}\right) \qquad 2$$

where i^o is the exchange current density, η is the overpotential for the reduction of reactant O, and α is the symmetry factor. In the reaction, only part of the overpotential activates the

forward reaction, and the symmetry factor represents the fraction of the overpotential affecting the forward reaction. All other parameters have their usual significance.

Most of the electrochemical reactions, however, are not elementary, especially for multiple electron transfer reactions. Even a 1-electron transfer reaction may involve several other steps. The whole reaction consists of multiple elementary reactions, including electron transfer steps and chemical steps. Each elementary reaction has a reaction rate. Each elementary step involving electron transfer gives a Butler-Volmer equation, and each chemical step gives a reaction rate equation. The whole reaction rate or electrochemical current is determined by the slowest step. Other steps also contribute to the whole reaction rate, depending on their reaction rates. Deduction of the whole reaction rate is complicated. In some cases, a chemical step is the rate determining step (rds). For example, in a carbon catalyzed ORR, adsorbed superoxide migration might be the rds. To simplify, for an electrochemical reaction involving multiple electron transfer, the rate determining step is considered a pseudo-elementary step with an electron transfer number of n. For ORR, n might be 1 or 2, depending on the catalysts used and the potential range. This pseudo-elementary step gives a current overpotential relationship, as shown in Equation (2), where *n* is the electron transfer number in the pseudo-elementary rate determining step, and α is the transfer coefficient representing the fraction of overpotential that activates the forward direction of the pseudo-elementary rate determining step.

A steady-state polarization curve describes the relationship between the electrode potential and the current density, which is recorded by either holding the electrode potential and recording the stable current response, or holding the current density and recording the stable potential response. The criteria to evaluate a polarization curve depend on its application. In fuel cells, for both ORR and fuel cell performance, high current density is expected at lower overpotential (ORR) or at higher cell voltage (fuel cell), which gives maximum power density. Fitting the polarization curves or plotting the overpotential vs. log (I) gives the Tafel slope and the exchange current density.

3.2.2 Cyclic voltammetry [39, 40]

Cyclic voltammetry is the most useful technique in electrochemistry. It can quickly provide qualitative information about catalysts and electrochemical reactions, such as the electrochemical response of catalysts and the catalytic activity of the catalysts with respect to some electrochemical reactions.

The common characteristic of all voltammetric techniques is that they involve the application of a potential (E) to an electrode and the monitoring of the resulting current (i) flowing through the electrochemical cell. In many cases the applied potential is varied or the current is monitored over a period of time (t). Thus, all voltammetric techniques can be described as some function of E, i, and t. They are considered active techniques (as opposed to passive techniques such as potentiometry) because the applied potential forces a change in the concentration of an electroactive species at the electrode surface by electrochemically reducing or oxidizing it.

The important parameters in a cyclic voltammogram (Figure 5) are the peak potentials (Epc, Epa) and peak currents (i_{pc}, i_{pa}) of the cathodic and anodic peaks, respectively. If the electron transfer process is fast compared with other processes (such as diffusion), the reaction is said to be electrochemically reversible, and the peak separation is

$$\Delta E\mathrm{p} = E\mathrm{pa} - E\mathrm{pc} = 2.303\, RT/nF \qquad (3)$$

The formal reduction potential (E^o) for a reversible couple is given by

$$\mathrm{E^o} = \frac{\mathrm{E_{pc}} + \mathrm{E_{pa}}}{2} \qquad (4)$$

For a reversible reaction, the concentration is related to peak current by the Randles–Sevcik expression (at 25 °C):

$$i_\mathrm{p} = 2.686 \times 10^5 n^{3/2} A c^0 D^{1/2} \mathrm{v}^{1/2} \qquad (5)$$

where i_p is the peak current in amps, A is the electrode area (cm^2), D is the diffusion coefficient ($cm^2\ s^{-1}$), c^0 is the concentration in mol cm^{-3}, and n is the scan rate in V s^{-1}.

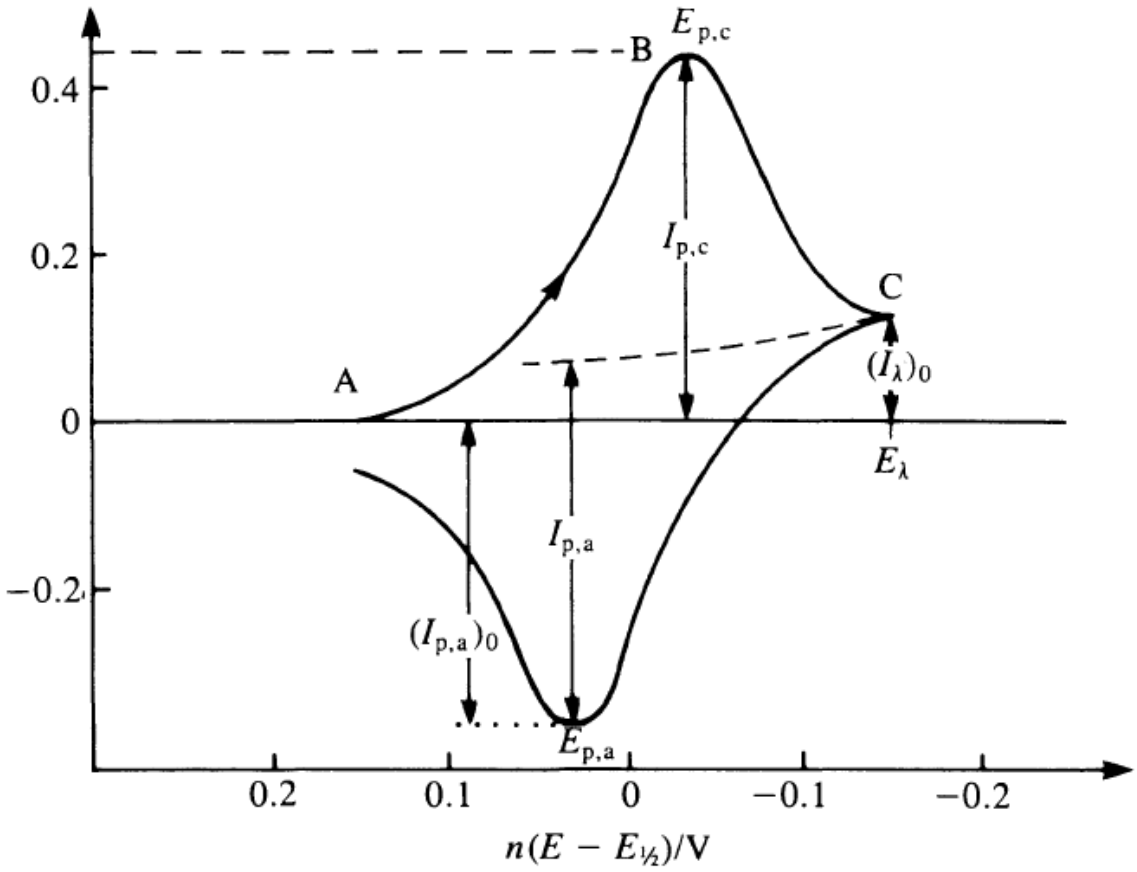

Figure 5 .Cyclic voltammogram for reversible systems

3.2.3 Hydrodynamic Voltammetry

In the hydrodynamic techniques the scanning of the potential takes place while the solution is in motion toward the electrode. In this way the solution closed to the Nernst (practically quiet) layer is continuously renewed. The motion is actuated in three different ways [41]:

- the electrode is stationary and the solution is stirred. This technique has low reproducibility and is practically not used.
- the solid electrode rotates around their own axis, the solution is than stirred. The electrode is a disk or a disk coupled with a ring.
- The solution flows into a tubular electrode at constant velocity. This system is used as voltammetric detector in HPLC.

Theory of Rotating Disc Voltammetry (RDV)

The rotating disk electrode (RDE) is one of the few convective electrode systems for which the hydrodynamic equations and the convective-diffusion equation have been solved rigorously for the steady state. This electrode is rather simple to construct and consists of a disk of the electrode material imbedded in a rod of an insulating material [42].

Unlike cyclic voltammetry which relies on the linear diffusion of species to the electrode surface. Rotating disk voltammetry provides much more quantitative information because electrolysis occurs under forced convection [42].

In a rotating disk experiment, the electrode is rotated at an angular velocity of ω, and the thin layer of electrolyte near the surface of the electrode acquires rotational momentum and spins out radially from the centre of the disk. The electrolyte at the surface is replenished by the upward flow as shown in Figure 6 below [42].

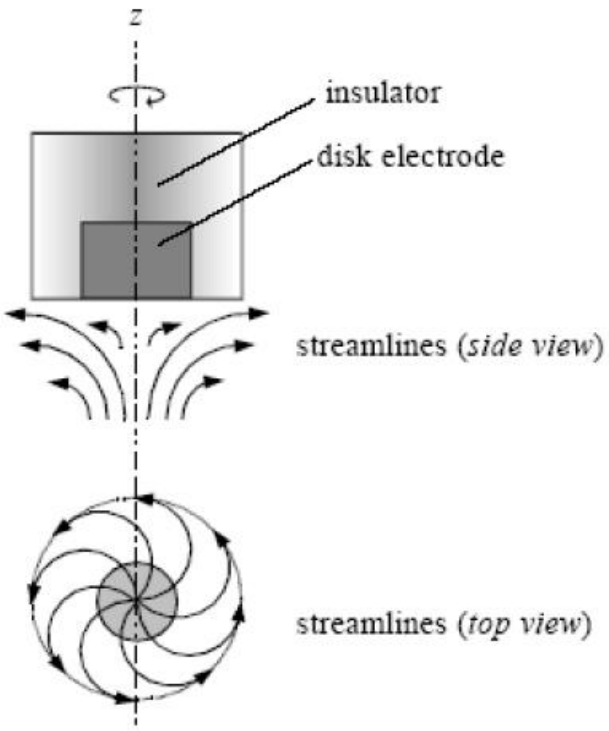

Figure 6. Sketch of a rotating disk electrode (RDE) with the schematic (top and side view) in the electrolyte. Z denotes the rotation axis.

The potential of the electrode is scanned linearly with time and the current response is recorded. The current is given by the following equation;

$$\frac{1}{i} = \frac{1}{i_k} + \frac{1}{i_L} \qquad (6)$$

$\frac{1}{i} = \frac{1}{i_k} + \frac{1}{i_L}$Where i is the observed limiting current, i_L is known as the Levich current given by;

$$i_L = 0.62nFAC_o D^{2/3} v^{-1/6} \omega^{1/2} \qquad (7)$$

Where C_o and D are the concentration and diffusion coefficient of the reactant in the electrolyte. v_k is the kinematic viscosity, A is the area of the electrode active surface and ω is the angular velocity of the electrode, and i_k is the kinetic contribution to the current given by

$$i_k = nFAC_o k^o \exp^{\frac{(-\alpha nF(E-E^o)}{RT}} = nFAk_f C\ \Gamma \qquad (8)$$

Where k^o is the standard heterogeneous rate constant, k_f is heterogeneous rate constant, Γ is surface coverage of electrode by active species and E^o is the formal potential. The surface coverage can be evaluated from the equation

$$\Gamma = Q/nFA \qquad (9)$$

At high overpotential, i_k is sufficiently large that the term $1/i_k$ becomes negligible and the limiting current is dominated by the mass transfer Levich current, i.e. $i=i_k$. A plot of i_L vs. $\omega^{1/2}$ yileds information about the diffusion parameter of the species in the electrolyte solution. The electrode current for case in mixed transport-kinetic control is described by both Equation (7) and (8). The combination of these equations produces the so-called Koutecky-Levich equation.

$$\frac{1}{i} = \frac{1}{i_k} + \frac{1}{i_L} = \frac{1}{nFAk_f C_o \Gamma} + \frac{1}{0.62nFAC_o D^{2/3} v^{-1/6} \omega^{1/2}} \qquad (10)$$

Hence, for cathodic reactions governed by mixed transport-kinetic control, plots of 1/i vs. $1/\omega^{1/2}$for constant values of k_f, i.e., fixed η, are predicted to generate straight lines having slopes proportional to 1/n and intercepts proportional to $1/k_f$. It is important to observe that the slopes of these plots are independent of applied overpotential.

In real systems, one also has to recognize the possibility of pores or pinholes in the film through which analyte can diffuse to the electrode [27]. A more general analysis involves

separating contribution of electron transfer from other limiting activity inside the film.Therfore the Koutecky-Levich equation can be expressed, assuming that the reaction in oxygen species is first order and that the electron transfer is the rate-determining step, as follows [43, 44]:

$$\frac{1}{|i|} = \frac{1}{\left|i^o\right|(\frac{\theta}{\theta_e})\exp^{-(\frac{\alpha nF}{RT})\eta}} + \frac{1}{\left|i_l^{fim}\right|} + \frac{1}{0.62nFD^{2/3}v^{-1/6}C_o\omega^{1/2}} \qquad (11)$$

$$= \frac{1}{\left|i^o\right|\exp^{-(\frac{\alpha nF}{RT})\eta}} + \frac{1}{\left|i_l^{fim}\right|} + \frac{1}{0.62nFD^{2/3}v^{-1/6}C_o\omega^{1/2}} \qquad (12)$$

where i_l^{diff} is the limiting diffusion current, i_l^{film} the limiting diffusion current in the catalytic film, i_k the kinetic current density, n the number of exchanged moles of electron per mole of oxygen, F the Faraday constant (96,485 C mol^{-1}), D_{O_2} the oxygen diffusion coefficient, v the kinematic viscosity, C_{O_2} the oxygen concentration in the considered electrolyte and ω is the rotation rate of electrode in rad s^{-1}. Equation 11 assumes that the electron transfer step is first order in adsorbed species and that of the backward reaction, oxygen evolution is quite negligible. Furthermore the adsorption process being rapind than the electron transfer step, one assume that $\theta = \theta_e$ at all electrode potential [44].

The diffusion limiting current, i_l^{diff}, of molecular oxygen in the bulk electrolyte is controlled by the rotation speed, ω, whereas the diffusion limiting current inside the film, i_l^{film}, is independent of ω. The diffusion limiting current in the electrolyte is given by the Levich's law;

$$i_l^{diff} = 0.62nFD^{2/3}v^{-1/6}C_o\omega^{1/2} \qquad (13)$$

Equation 12 shows that the plot of the inverse of the current, corrected from the background current is a linear function of $\omega^{-1/2}$. The slope of the straight line leads to the total number of exchanged electrons and the intercept at the origin gives the inverse of the kinetic current, i_k, corrected from the diffusion current, as function of the over voltage, i.e

$$\frac{1}{i_k} = \frac{1}{\left|i^o\right|\exp^{|\eta/b|}} + \frac{1}{\left|i_l^{fim}\right|} \qquad (14)$$

Equation (14) thus shows that for high overvoltage ($|\eta| \rightarrow \infty$) the quantity $1/ i_K$ tends towards $1/ i_l$, so that one can obtain the limiting current density i_l by extrapolating eq. (34) at high η.This allowed as to transform Equation (14) as follows: [43, 44]

$$\eta = -b(\ln\left|\frac{i_k}{i_l - i_k}\right| + \ln\left|\frac{i_l}{i^o}\right|) \qquad (15)$$

$$\eta = -\frac{1}{\alpha nf}(\ln\left|\frac{i_k}{i_l - i_k}\right| + \ln\left|\frac{i_l}{i^o}\right|)$$

Plotting $1/i_k$ as a function of electrode potential E, allowed as determining limiting current (i.e. resulting from a mixed control inside the polymer). Knowing i_l it is possible to plot ln [i_k / (i_k - i_l)] vs the over potential η gives a straight line with a slope 1/ b and an intercept at the origin [-ln (i_l / i^o)]. From this results Tafel slope (b) and i^o can be calculated [43]. The slope (b) of Tafel plot at 25^{o}C is

$$-b = -\frac{1}{\alpha nf} = -\frac{RT}{\alpha nF} \qquad (16)$$

3.3 Electrochemical Process

3.3 1 Three Electrode Systems

Voltammetry experiments investigate the half cell reactivity of an analyte. Most experiments control the potential (volts) of an electrode in contact with the analyte while measuring the resulting current. In most electrochemical techniques, there are three electrodes—the working electrode, the reference electrode and the counter (or auxiliary) electrode. The three electrodes are connected to a potentiostat, an instrument that controls the potential of the working electrode and measures the resulting current.

There are many systems which have more electrodes, but their design principles are generally the same as the three electrode system. For example, the rotating ring-disk electrode has two distinct and separate working electrodes, a disk and a ring, which can be used to scan or hold potentials independently of each other. Both of these electrodes are balanced by a single reference and auxiliary combination for an overall four electrode design. More complicated experiments may add working electrodes as required and at times reference or auxiliary electrodes [35, 40, 41]

A. Reference Electrodes

The reference electrode should provide a reversible half-reaction with Nernstian behavior, be constant over time, and be easy to assemble and maintain. The most commonly used reference electrodes for aqueous solutions are the calomel electrode, with potential determined by the reaction $Hg_2Cl_2(s) + 2e– = 2Hg(l) + 2Cl–$ and the silver/silver chloride electrode (Ag/AgCl), with potential determined by the reaction $AgCl(s) + e– = Ag(s) + Cl^–$ These electrodes are commercially available in a variety of sizes and shapes.

B. Working Electrode.

It is the electrode at which the reaction of interest occurs. The performance of the voltammetric procedure is strongly influenced by the working electrode material. A wide range of solid materials are used as electrodes. The most common 'inert' solid electrodes are lead, vitreous carbon (glassy carbon), gold and platinum.

C. Counter Electrode

It is an electrode which supply the current required by the working electrode with out limiting the measurement response of the cell. It is the current carrying electrode and must be inert and larger in dimension. Platinum wire or foil is the most common counter electrode.

3.3.2 Supporting Electrolyte

Normally electrode reactions take place in solutions, or sometimes in molten salts. In order to minimize the phenomenon of migration of the electroactive ions caused by the electric field and to confine the interfacial potential difference to the distance of closest approach of solvated ions to the electrode, the addition of a solution containing a high concentration of inert electrolyte, called supporting electrolyte, is necessary. This has a concentration at least 100 times that of the electroactive species and is the principal source of electrically conducting ionic species. The supporting electrolyte should be chosen, as well as its concentration, so that the transport numbers of the electroactive species are practically zero: it can be an inorganic or organic salt, an acid or a base, or a buffer solution such as citrate, phosphate, or acetate. The choice also has to be made in relation to the properties of the solvent employed [42].

All care must be taken to ensure that the supporting electrolyte is truly inert in the potential range of the experiment, not reacting with the electrode or with the products of the electrode reaction (except when desired).

3.3.3 Removal of Oxygen

Removal of oxygen in the laboratory solutions can be done by saturated with an inert gas that reduces the partial pressure of oxygen to a very low value. Inert gases employed are nitrogen and argon: the latter has the advantage of being heavier than air and not escaping easily from the cell, whereas the former is lighter than air; however, nitrogen is much less expensive than argon. Gas purity is very important, and ultra-pure gases should always be preferred [42].

3.4 Objectives of the Studies

- To prepare electrochemically and characterize poly(1, 8-DAN) and polypyrrole on GC and MWCNT modified GC electrode
- To study the electrocatalytic activity of poly(1, 8-DAN) and polypyrrole on GC and MWCNT modified GC electrode
- To calculate the kinetic parameter of oxygen reduction reaction on GC/MWCNT/ poly (1, 8-DAN) electrode on different cycles of deposition from the rotating disc voltammograms

4. Experimental Section

4.1 Chemicals Used

All chemical and reagents used were analytical grade, 0.05 µm Al_2O_3 was used for polishing the electrode surface. The supporting electrolyte used for electrochemical method was 0.2 M Na_2SO_4 (pH = 1) solution. Multiwall carbon nanotubes were used as received. 1, 8 – Diaminonaphthalene, and pyrrole, were used to prepare the monomer solution. Distilled water was used to prepare the electrolyte solution.

4.2 Pretreatment of MWCNT and Preparation of GC/MWCNT Modified Electrodes

The MWCNT was functionalized to introduce oxygen-containing functional groups on the MWCNT surface. For functionalization or surface oxidation, MWCNTs were mixed with a 1:1 mixture of 98% H_2SO_4 and 70% HNO_3. Approximately 50 mg of MWCNT were added to 24 mL of the acid mixture in a round bottom flask . The mixture was refluxed for two hours at 55^oC and then for three hours at 80^oC. Afterwards, the nanotubes were washed with distilled water by centrifugation for several times until the filtrate became neutral. Finally, the MWCNTs were dried under vacuum for 15 hours [35]. This procedure shortened the nanaotubes, produced carboxylic acid and hydroxyl groups mainly on the open ends as well as the sidewalls, thus introduced negative charges to MWCNTs and improved the dispersion in water [35].

1.0 mg acid treated MWCNTs were dispersed into 1 ml of distilled water and sonicated for 30 min to give a homogeneous black suspension. About 5 µL of the suspension was cast on the polished GC electrode surface using a micropipette and dried in air at room temperature [43].

4.3 Electrochemical Measurement

A three electrode system was used for voltammetric measurements. Electrochemical experiments were carried out using Epsilon Electrochemical Workstation. A glassy carbon electrode (area: 0.0707 cm^2) or modified GC electrode were used as a working electrode, while a platinum wire and Ag/AgCl (sat'd KCl) were used as auxiliary and reference electrodes, respectively. The GC electrode was polished to a mirror finish with 0.3-0.5 µm

alumina powder, rinsed with water, and dried before each experiment. O_2 saturated and Ar saturated 0.2 M Na_2SO_4 solution was used as the electrolyte. Rotating disk experiments were performed at different rotation speed between 100 rpm and 1600 rpm.

4.4 Preparation of Modified Electrodes

Before the preparation of the modified electrode, GC electrode was mechanically polished to a mirror finish using polishing pad containing 0.05 µm alumina powders and carefully cleaned with water. Then the electrodes were cycled in 0.2 M Na_2SO_4 (pH=1) solution in a potential range from -0.8 V to 0. 8 V at a sweep rate 100 mV/s in order to check the cleanliness of the system. MWCNTs modified GC electrode was prepared by casting 5 µL aqueous dispersed MWCNTs suspension and dried in air at room temperature. These modified electrodes used for electrochemical deposition of the polymer film [43].

The electrochemical deposition of 1, 8-Diaminonaphthalene was carried out by cyclic voltammetry between -0.4 V and 1.4 V on GC electrode and between -0.4 to 0.8 V on MWCNT/GC electrode for different cycles (5, 8 and 12 cycles on MWCNT/GC). The polypyrrole film was electrochemically prepared on GC and MWCNT/GC electrodes by cycling the potential between -0.6 V to 1.0 V at a scan rate of 50 mV/s. The resulting films were then washed with distilled water. Finally, the modified GC electrodes were cycled between -0.8 V to 0.8 V in 0.2 M Na_2SO_4 until a stable voltammogram is obtained [43-45].

5. Result and Discussion

5.1 Electrochemical Polymerization of 1, 8-Diaminonaphthalene

The electropolymeriaztion of 1, 8-DAN was carried out from a solution of 1 mM 1, 8-DAN in a 0.1 M HCl by cycling the potential between -400 mV and 800 mV on GC and -400 mV-1400 mV on GC/MWCNT electrode at 50 mV/s. A thin films made with 5 and 8 deposition cycles were used. A comparison of the cyclic voltammetric growth profile of poly (1, 8 – DAN) at GC and MWCNT/GC electrode is depicted in Figure 7.

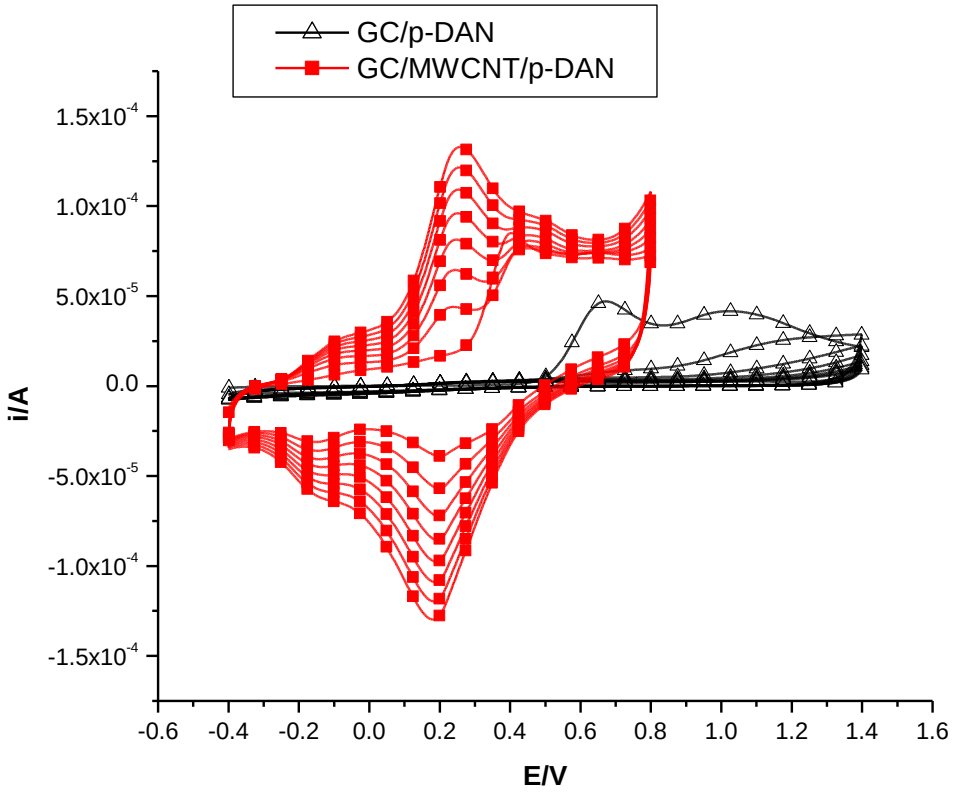

Figure 7. Cyclic voltammograms for the electropolymerization of 1, 8-DAN on GC (△) in the potential range of -0.4 V to 1.4 V and MWCNT (■) in the potential range of -0.4 V to 0.8 V at a scan rate of 50 mV/s.

The monomer was first oxidized with a large anodic current peak with its peak potential at about 0.66 V at GC and 0.41 V at MWCNT/GC, which was followed by the growth of the polymer with the monomer oxidation peak suppressed in subsequent potential cycles. This is a typical behavior for autocatalytic growth of conducting polymers, in which the oxidized

polymer acts as an electrocatalyst for taking electrons away from the monomer molecules, leading to the polymer growth [43]. On scanning to negative potential, no characteristic cathodic peak appeared at GC electrode. But at GC/MWCNT, the reduction peaks are clearly observed. The monomer is more easily oxidized at GC/MWCNT electrode (E_p= 224 mV) than GC electrode (E_p = 490 mV). The peak current, I_p for the oxidation of the monomer is six times higher at the MWCNT/GC than at GC electrode.

Electrochemical Behavior of GC/ poly (1, 8-DAN) and GC/MWCNT/ poly (1,8-DAN) Modified Electrode

The cyclic voltammograms of the polymer modified electrodes were recorded in monomer free electrolyte solution (Figure 8). Like the facile oxidation of the monomer resulting in a rapid growth of polymer at the GC/MWCNT, the polymer redox process was also found to be more facile at GC/MWCNT.

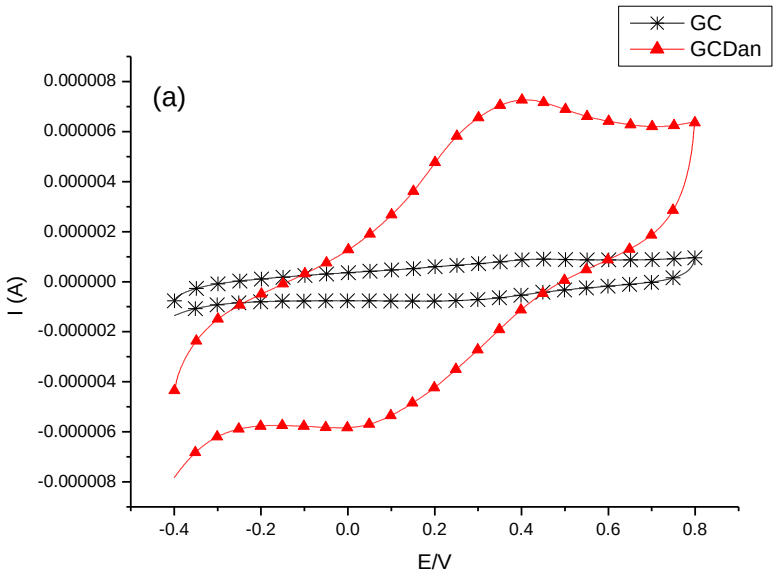

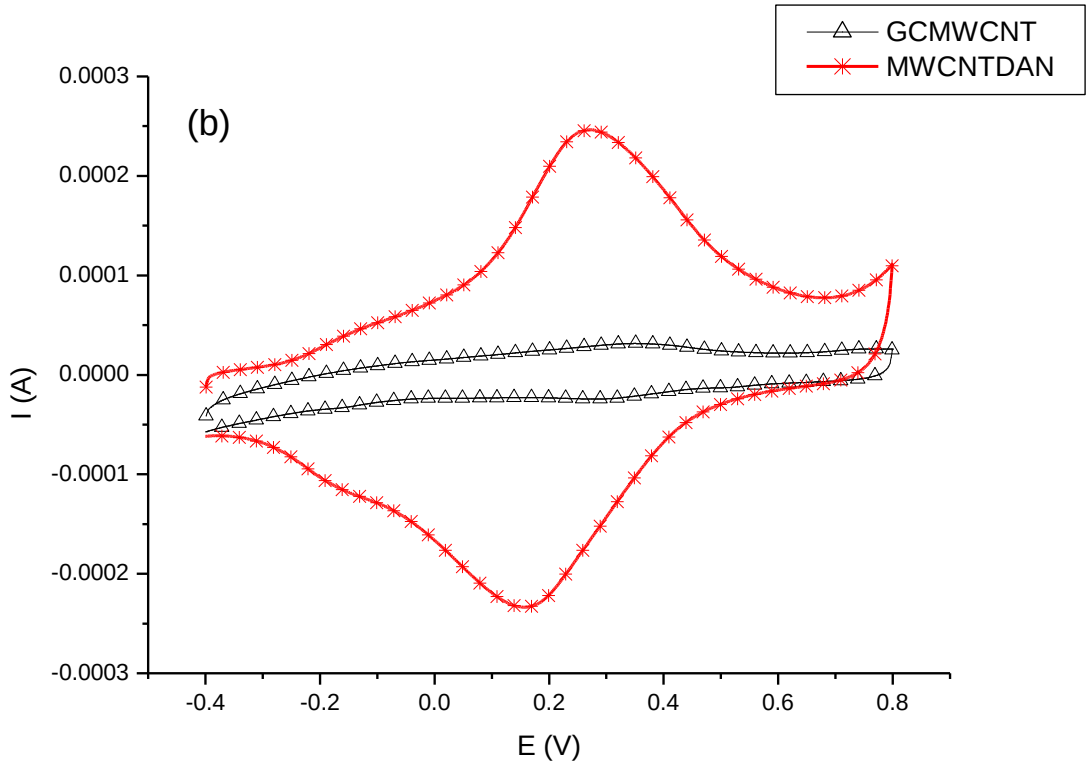

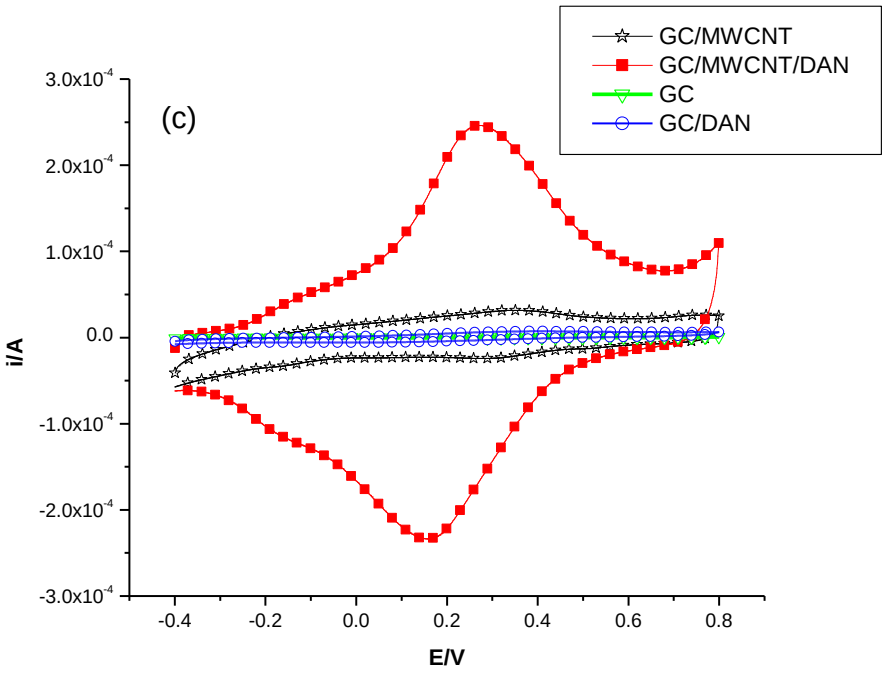

Figure 8. Cyclic voltammograms of poly (1, 8 – DAN) at 50 mV/s in monomer free 0.2 M Na_2SO_4 at pH 1; (a) GC (✳) and GC/ poly (1,8-DAN) (▲) (b) GC/MWCNT (△) and GC/MWCNT/ poly (1,8-DAN) (✳) (c) the overlay of cyclic voltammograms of GC(▼), GC/p-DAN (○) , GC/MWCNT (◀) and GC/MWCNT/p-DAN (■).

The oxidation potential of the polymer was 382 mV at GC/ poly (1, 8-DAN) and 262 mV at GC/MWCNT/ poly (1, 8-DAN) and favorably shifted by about 120 mV. The total charge passed during polymerization for the first 8 cycles at GC and MWCNT/GC electrode was found to be 7.75 μC and 242.63 μC, respectively. This unique enhancement in the redox charge of the polymer deposited on the MWCNT/ GC electrode is another indication of a strong interaction between the polymer and carbon nanotubes.

Figure 9 shows the cyclic voltammograms of poly (1, 8-DAN) at GC/MWCNT electrode of various thickness (5, 8 and 12 cycles). To estimate the amount of poly (1, 8- DAN) in GC/MWCNT electrodes, the real surface area of polymer was detrmined by charge integration under the reduction peak of the polymer corrected for the base line. The charge under the cathodic reduction peak (Q_c) and anodic oxidation peak (Q_a) for three MWCNT/poly (1, 8-DAN) modified GC electrode was detrmined (Table 2). The value of Q_c and total area incresed with increasing the number of coating cycles.

Table 2. Vlaues of the anodic and cathodic charges passed through GC/MWCNT/ DAN at different number of depostion cycles.

Number of depostion cycles	Peak potential (mV)	Peak current (μA)	Q_a ($x10^{-5}$ C)	Q_c ($x10^{-5}$ C)	Surface coverage (Γ) x 10^{-9} mol/cm^2
5 cycles	256	187.94	6.726	7.211	5.286
8 cycles	292	235.32	10.110	9.228	6.764
12 cycles	290	324.65	14.422	12.761	9.353

The anodic and cathodic charges are close in value; suggesting that the same amount of charges passed in both the forward and reverse scan and the oxidation and reduction of the polymer might be reversible.

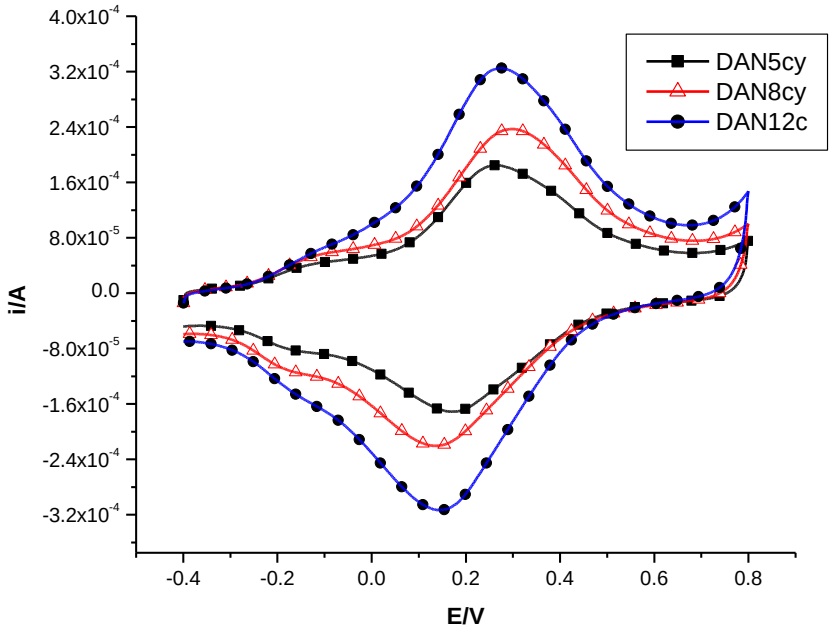

Figure 9. Cyclic voltammograms for GC/MWCNT electrodes coated with 5 cycles of poly (1, 8-DAN) (■), 8 cycles poly (1, 8-DAN) (△) and 12 cycles of poly (1, 8-DAN) (●) in 0.2 M Na_2SO_4 (pH=1) solution at scan rate of 50 mV/s.

5.2 Electrochemical Polymerization of Pyrrole

Figure 10 shows the cyclic voltammogram recorded during the electroplymeriaztion of 25 mM pyrrole solution. The peak current increased as the cycle numbers increased, indicating the formation and growth of a polymer on the glassy carbon electrode.

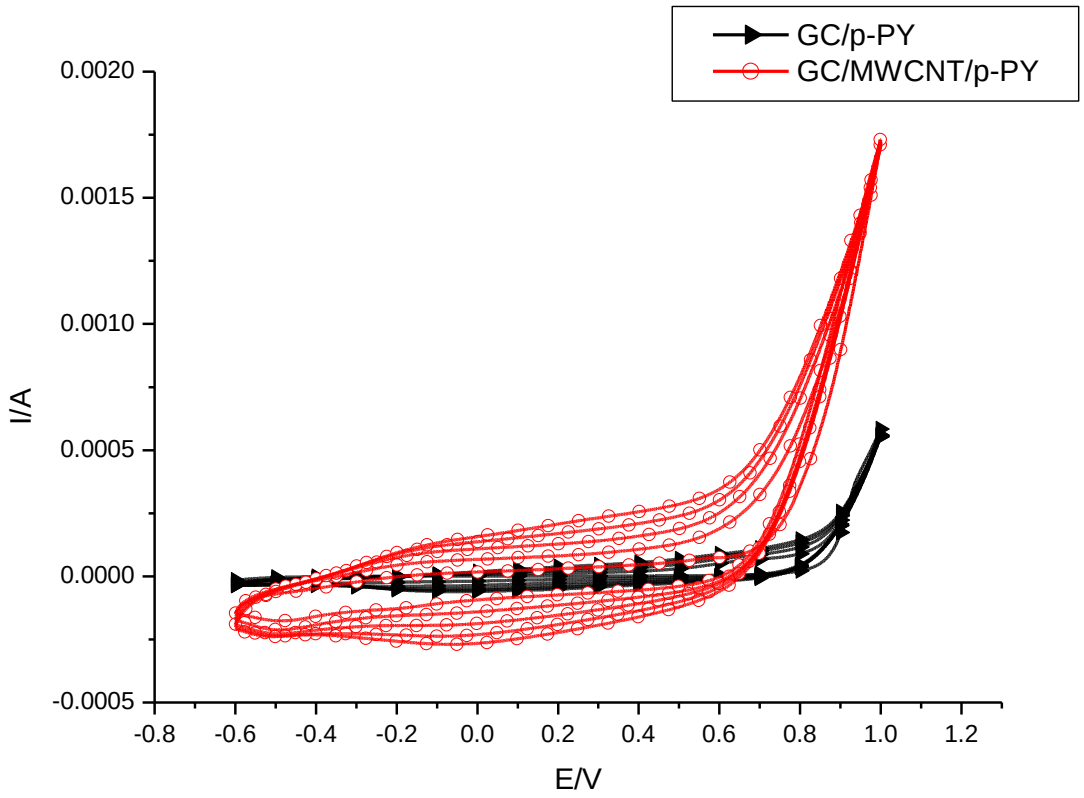

Figure 10. The cyclic voltammograms recorded for the electropolymerization of polypyrrole from a solution containing pyrrole monomer in potential range of -0.6 to 1 V at 50 mV/s at GC (○) and GC/MWCNT (▶) electrodes.

On the first anodic scan, a single anodic wave was typically observed at relatively high potential of about 690 mV (at GC/MWCNT) and 870 mV (at bare GC). This is consistent with oxidation of pyrrole monomer to produce the radical cation [47]. With each successive scan, the peak current associated with both the anodic and cathodic waves of the polymer increased consistent with the growth of the polymer film. Enhanced growth of the polymer was observed on GC/MWCNT and similarly the monomer was easily oxidized on MWCNT/GC electrode (oxidation peak was shifted cathodically by about 180 mV).

The cyclic voltammograms recorded for polypyrrole-coated GC/MWCNT cycled in the monomer-free electrolyte solution are presented in Figure 11.

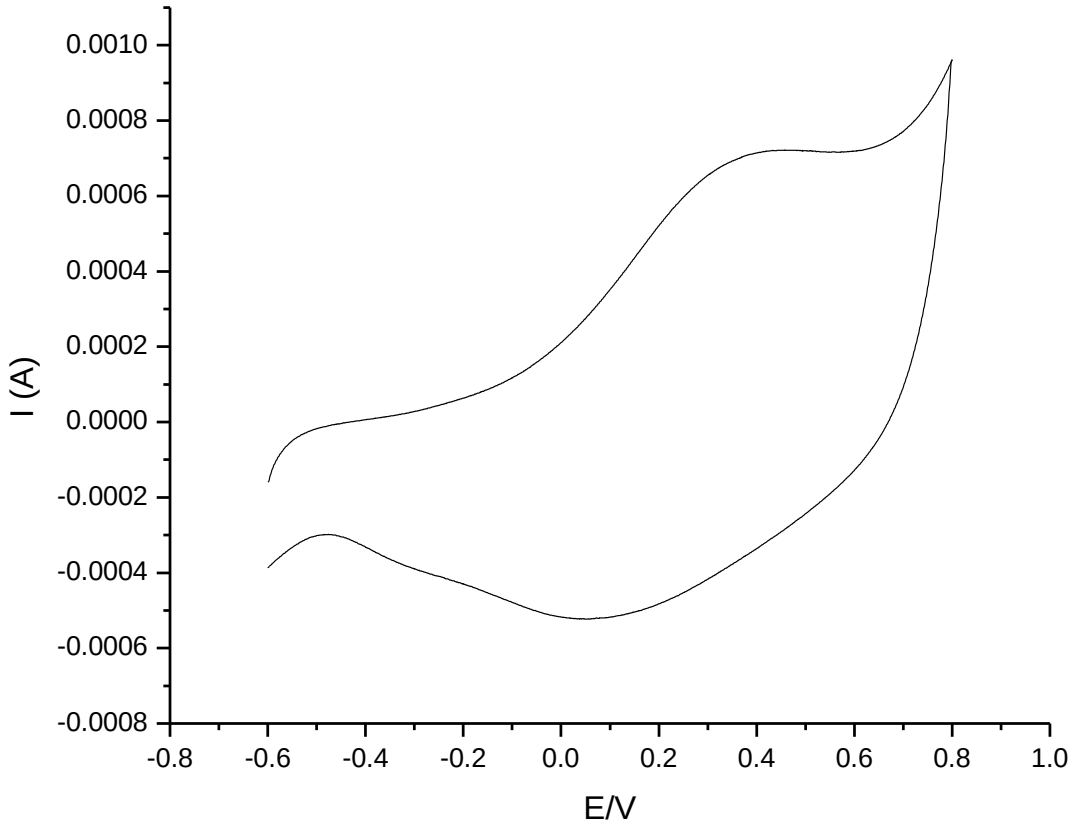

Figure 11.Cyclic voltammogram of polypyrrole at 50 mV/s in monomer free solution.

5.3 Cyclic Voltammetric Investigation of the Electrocatalytic Reduction of Oxygen

Cyclic voltammetry is an effective and convenient method for probing the electrochemical features of the modified electrode surfaces. The electrochemical reduction of oxygen has been carried out at GC, MWCNT/GC, poly (1, 8-DAN)/MWCNT/GC, and polyppyrrole/MWCNT/GC modified electrode at sweep rate of 10 mV/s.

Electrocatalytic Reduction of Oxygen at MWCNT/p-DAN Modified GC Electrode

The electrocatalytic activity of GC/MWCNT/p-DAN for oxygen reduction was investigated by cyclic voltammetry and compared with GC, GC/MWCNT, and GC/p-DAN. Figure 12 shows the cyclic voltammograms recorded for oxygen reduction at GC, GC/MWCNT. The MWCNT –modified electrode has a very large background current compared with bare GC due to the significant increase of the electrode surface area. At GC, the cyclic voltammogram shows an ill-defined reduction peak at potentials greater than -350 mV. At MWCNT/GC, the cyclic voltammogram shows the oxygen reduction peak at -153 mV. The oxygen reduction potential for the MWCNT/GC electrode is shifted by about 197 mV with a nearly 2 times increase in current compared to GC electrode.

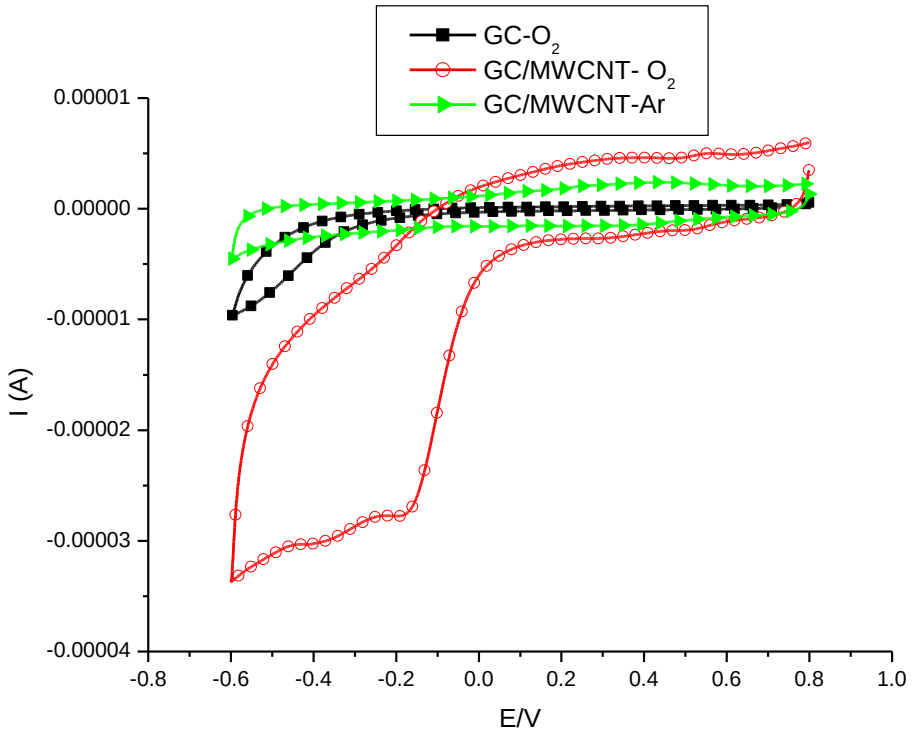

Figure 12. Cyclic voltammograms for the reduction of dissolved oxygen in 0.2 M Na_2SO_4 at pH 1 at GC (■), GCE/MWCNT (○) and in Ar saturated solution at GCE/MWCNT (▶) at 10 mV/s .

Figure 13 shows the cyclic voltammograms of 0.2 M Na_2SO_4 soltuion (pH = 1) saturated with O_2 at GC/MWCNT (✳) and GC/MWCNT/p-DAN (△) modified electrodes. The

cathodic peak at 153 mV (for GC/MWCNT) and 160 mV (for GC/MWCNT/p-DAN) corresponds to the electrochemical reduction reaction of oxygen at scan rate of 20 mV/s. The enhanced electrocatalytic effect of GC/MWCNT/p-DAN over GC/MWCNT can be clearly observed from two important features; the positive shifit of the O_2 reduction potential and an increase in the oxygen reduction peak current.

All the above result indicated that the GC/MWCNT/p-DAN modified electrode has good electrocatalytic activity for the electrochemical reduction rection of oxygen.

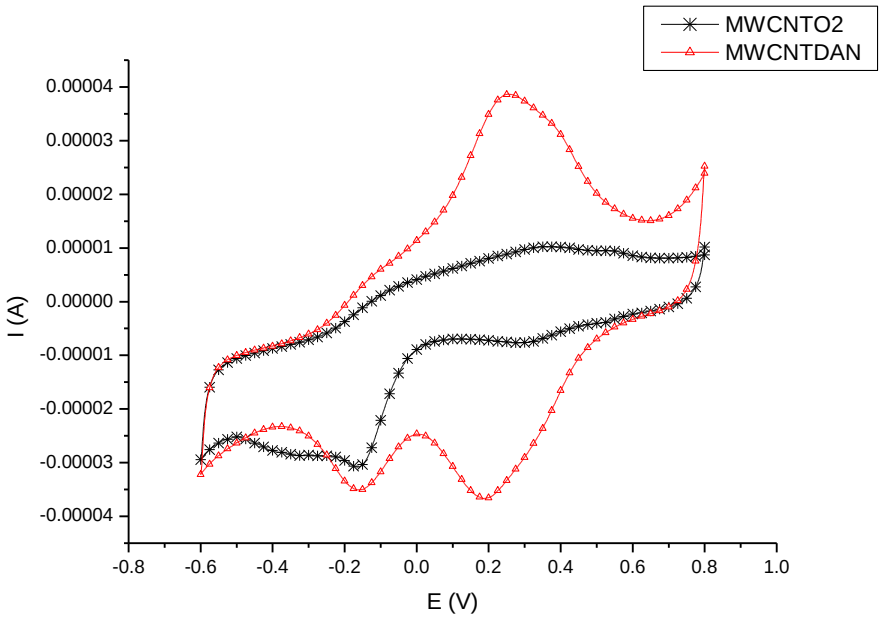

Figure 13. Cyclic voltammograms for the reduction of dissolved oxygen in 0.2 M Na_2SO_4 at pH 1 at 10 mV/s (✳) GC/MWCNT and (△) GC/MWCNT/p-DAN modified electrode.

5.3.2 Electrocatalytic Reduction of Oxygen at MWCNT/polypyrrole Modified GC Electrode

The catalytic activity of the electrocatalyst GC/MWCNT/p-Py for oxygen reduction reaction was tested using cyclic voltammetry. Figure 14 shows the cyclic voltammograms of 0.2 M Na_2SO_4 solution (at pH=1) saturated with argon (◆) and with oxygen (▶) at GC/MWCNT/p-Py modified electrode. From Figure 14, no significant electrocatalytic reduction of molecular oxygen was observed at p -PY/MWCNT modified GC electrode.

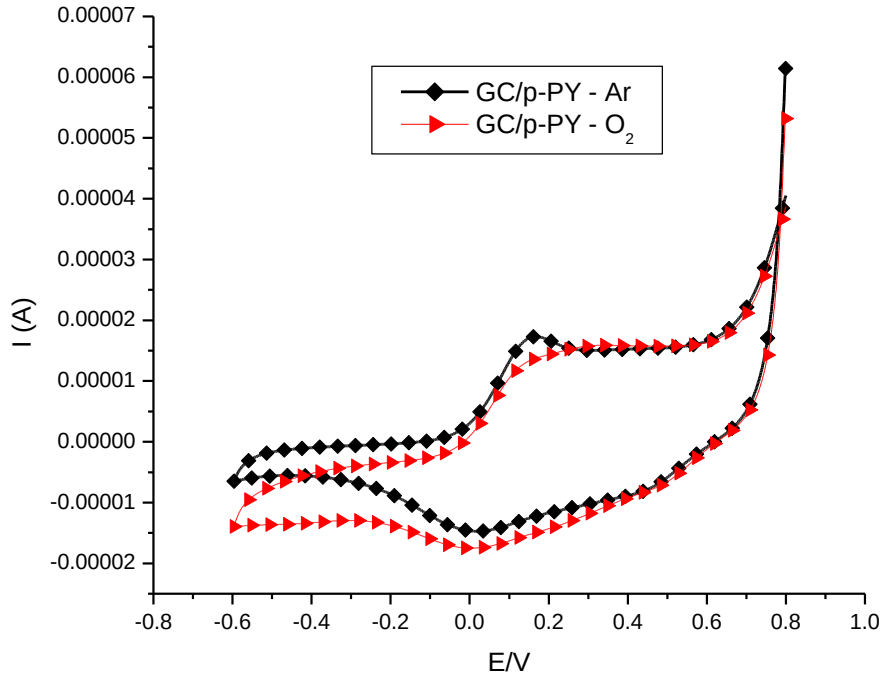

Figure 14 .Cyclic voltammograms for GC/MWCNT/p-Py electrodes Ar saturated (◆) 0.2 M Na_2SO_4 solution (at pH=1) and O_2 saturated (▶) 0.2 M Na_2SO_4 solution (at pH=1) at scan rate of 20 mV/s.

5.4 Rotating Disk Electrode Investigation of the Electrocatalytic Reduction of Oxygen

Electrocatalytic activity of the modified electrodes towards oxygen reduction was explored using the rotating disk electrode method.

5.4.1 Oxygen Reduction at MWCNT/ p-DAN (5 cycles) Modified GC Electrode

The reduction of oxygen at GC/MWCNT/p-DAN was investigated using a rotating disk electrode (RDE). Electrode rotation rate between 100 and 1600 rpm were used and the resulting voltammograms are given in Figure 15.

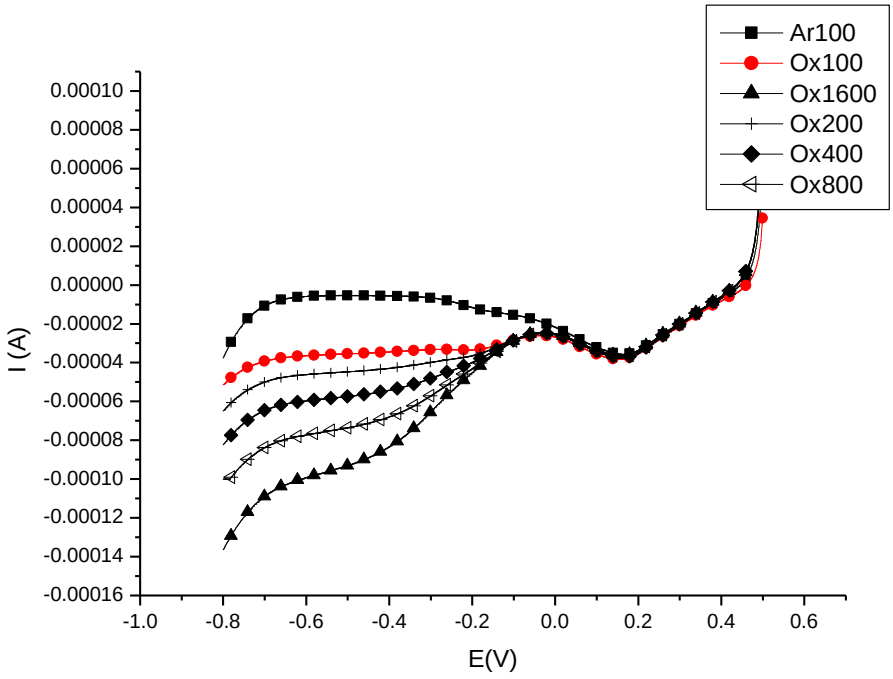

Figure 15. Rotating disk voltammograms at different rotation rates recorded at GC/MWCNT/p-DAN in O_2 saturated 0.2 M Na_2SO_4 electrolyte at pH 1; (■) in the absence of O_2 and at different rotating rates in the presence of O_2; 100 (●), 200 (+), 400 (◆), 800 (◁), 1600 (▲) rpm.

In Figure 15 the onset reduction was observed at about -0.098V vs Ag/AgCl and plateau region was observed. The current of oxygen reduction increases at a given potential with the increase of the rotation rate. The Levich plot, i_L vs. $\omega^{1/2}$ for oxygen reduction reaction at GC/MWCNT/p-DAN modified electrode in O_2 saturated 0.2 M Na_2SO_4 (pH=1) solution are shown in Figure 16. A good linear (R= 0.9992) response is observed, which suggests that the oxygen reduction reaction is limited by diffusion control [41]. The Levich plot was compared to calculated line for a two-electron and four-electron process and close to four-electron transferred process (Figure 17).

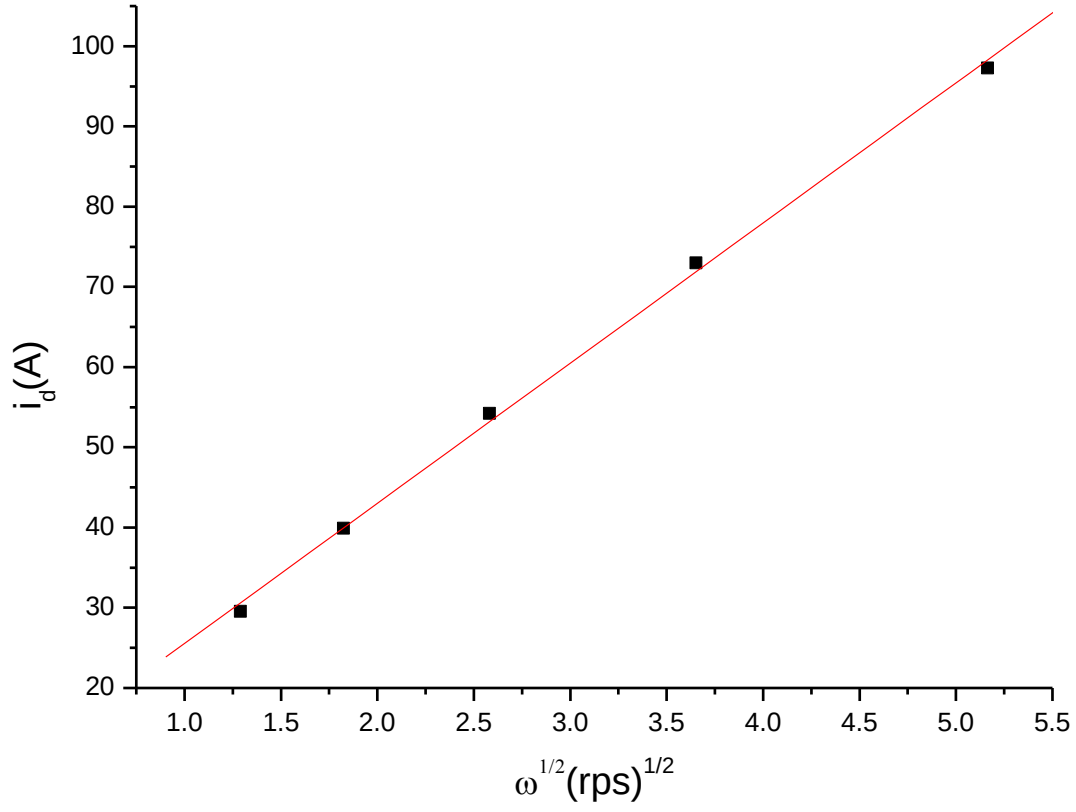

Figure16. Levich plot of limiting currents at -0.68 V *vs* Ag/AgCl for reduction of oxygen at GC/MWCNT/p-DAN modified electrode at O_2 saturated 0.2 M Na_2SO_4 (pH= 1) solution.

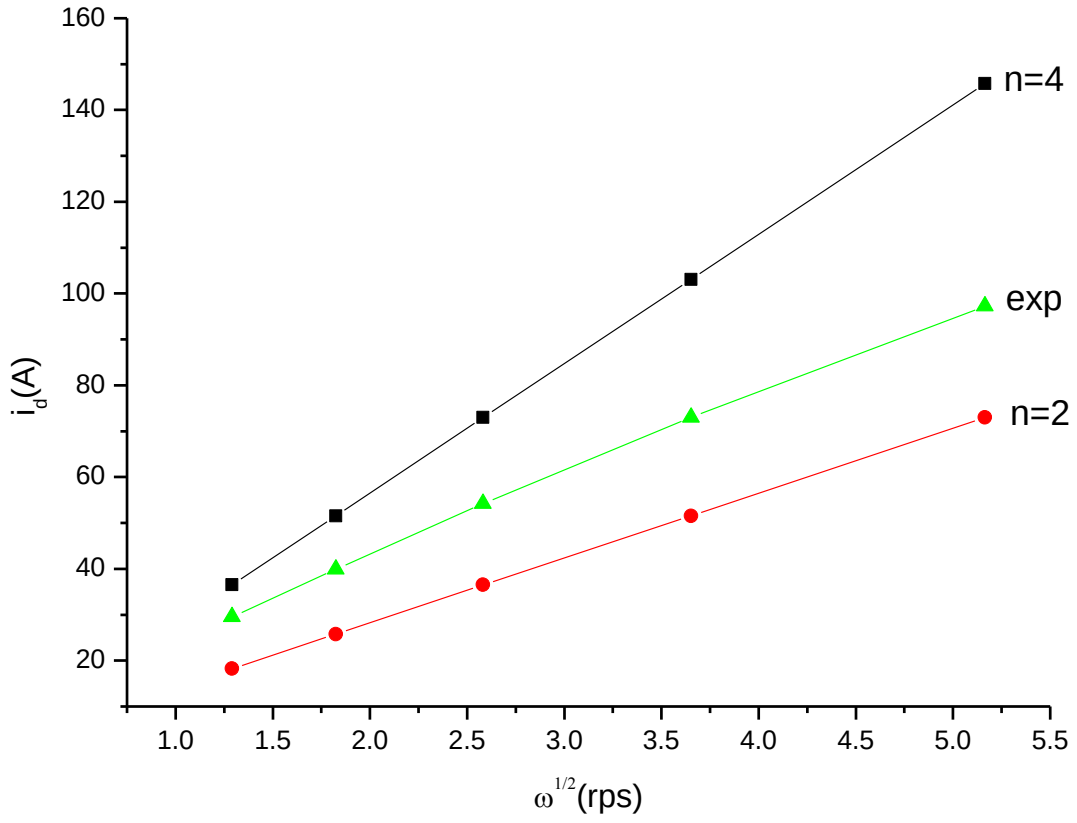

Figure 17. Levich plots for the reduction of oxygen at MWCNT/p-DAN modified glassy carbon electrode (O_2 saturated 0.2M Na_2SO_4,10mV/s) for theoretical (2es and 4es) and experimental result.

Figure 18 shows the Koutecky-Lecich plots obtained from the RDE data. Linear K- L plots are observed and from the slope of these lines the number of electrons transferred per O_2 molecule was (found to be 3.7) which indicates the direct reduction of O_2 to H_2O. The slope of the experimental plot (0.03812 µA $(rps)^{-1/2}$) agrees reasonably well with the theoretical value (0.0354 µA $(rps)^{-1/2}$) for the four electron process.

The rate constant for the ORR at GC/MWCNT/p-DAN was determined from K-L plot using Equation 8. From the intercept of the K-L plot (Figure 12) and surface coverage (Γ) from Table 2, the rate constant for the ORR was determined as 1.499 x 10^3 $M^{-1}s^{-1}$.

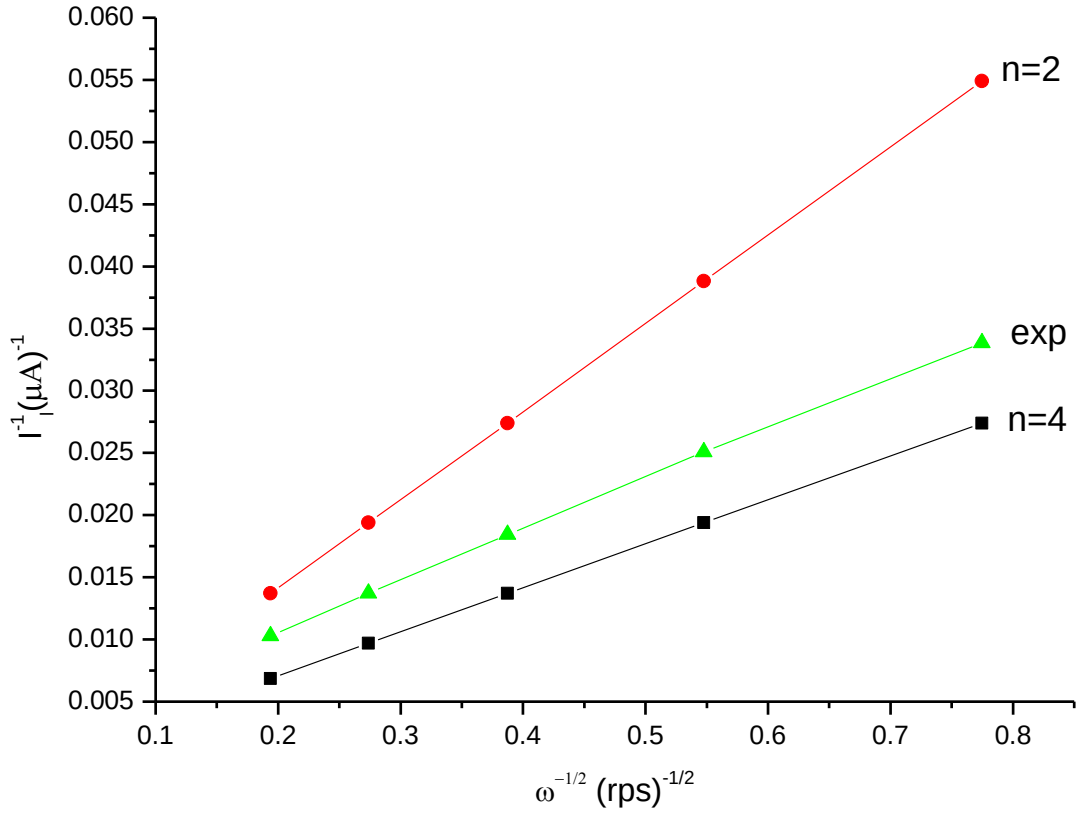

Figure 18. Koutecky –Levich plot of i^{-1} vs $\omega^{-1/2}$ for reduction of oxygen on GC/MWCNT/p-DAN rotating disk electrode for O_2 saturated 0.2 M Na_2SO_4 solution

Koutecky –Levich plots i^{-1}*vs* $\omega^{-1/2}$ (with data taken from Figure 15) at various potential (Figure 19) yields straight lines. The slope of these straight lines remains almost constant over the potential range of -0.34 V to -0.7 V. This indicates that a constant numbers of electrons are involved in the reduction reaction [42]. The slopes of these straight lines yielding the number of electrons transferred are four and the intercept of which at the origin giving i_k^{-1}.

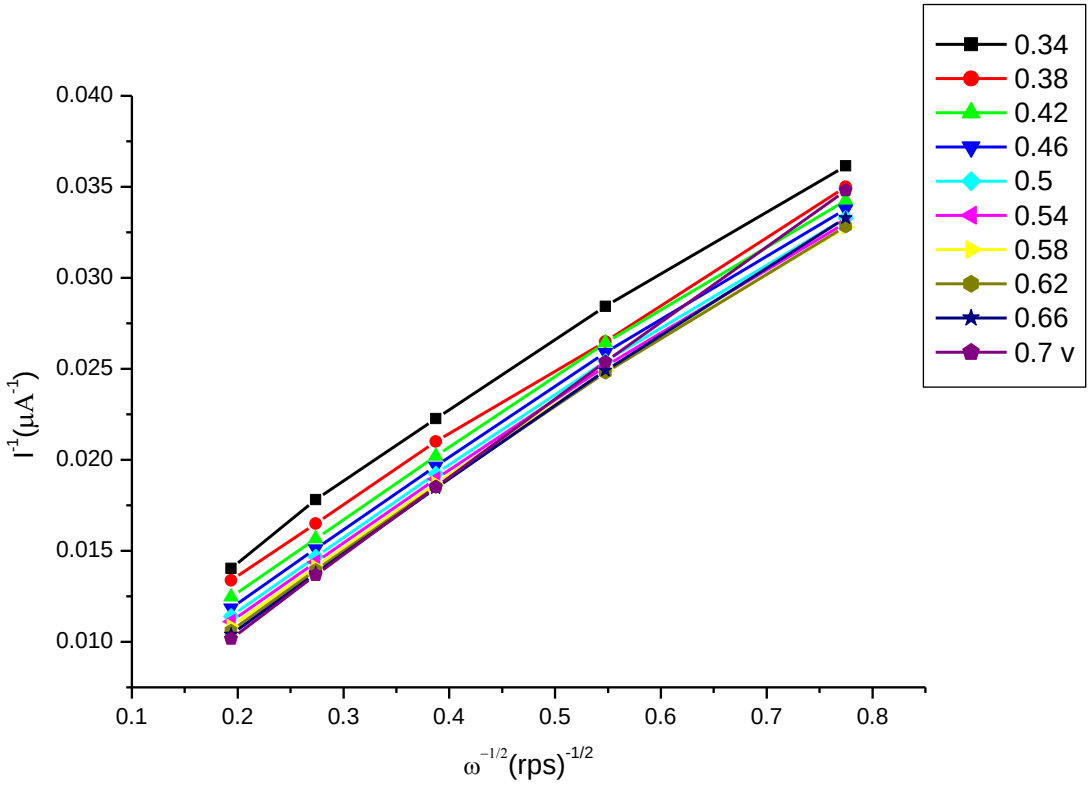

Figure 19.Koutecky-Levich plot for the reduction of oxygen on GC/MWCNT/p-DAN rotating disk electrode at different potentials.

From Figure 19, the plot of i_k *vs* E are drawn and gives a linear curves (Figure 20). Figure 20 shows that when the potential become more negative, the kinetic limiting current (i_k) increases. It indicates that the more negative potential would be more favorable for electron transfer process.

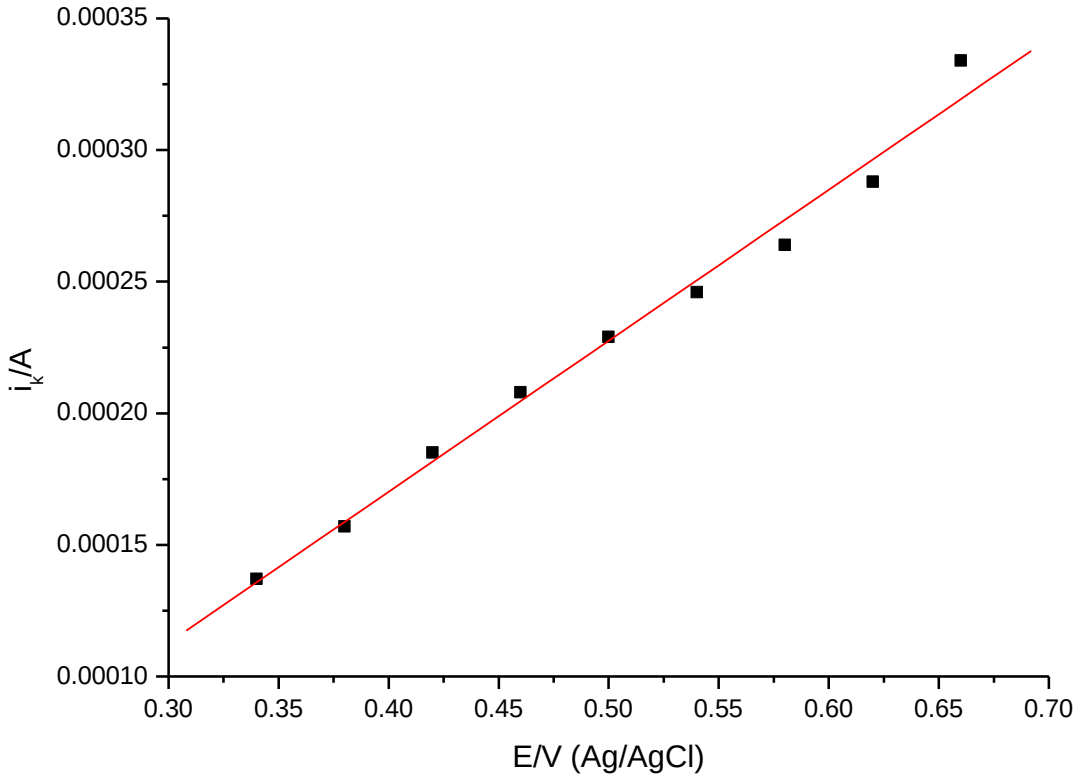

Figure 20. Plot of i_k vs E for reduction of oxygen on GC/MWCNT/p-DAN rotating disk electrode for O_2 saturated 0.2 M Na_2SO_4 solution

Equation 12 shows that for high overvoltage ($|\eta| \rightarrow \infty$) the quantity i_k^{-1} tends towards i_l^{-1}, so that one can obtain the limiting current by extrapolating Equation 12 at high η. The plot of $1/i_k$ (from the intercept of K-L plots) as the function of the electrode potential is shown in Figure 21. The value of $1/i_L$ obtained was 3230 A^{-1} and i_l for GC/MWCNT/p-DAN modified electrode was found to be 3.098 x 10^{-4} A.

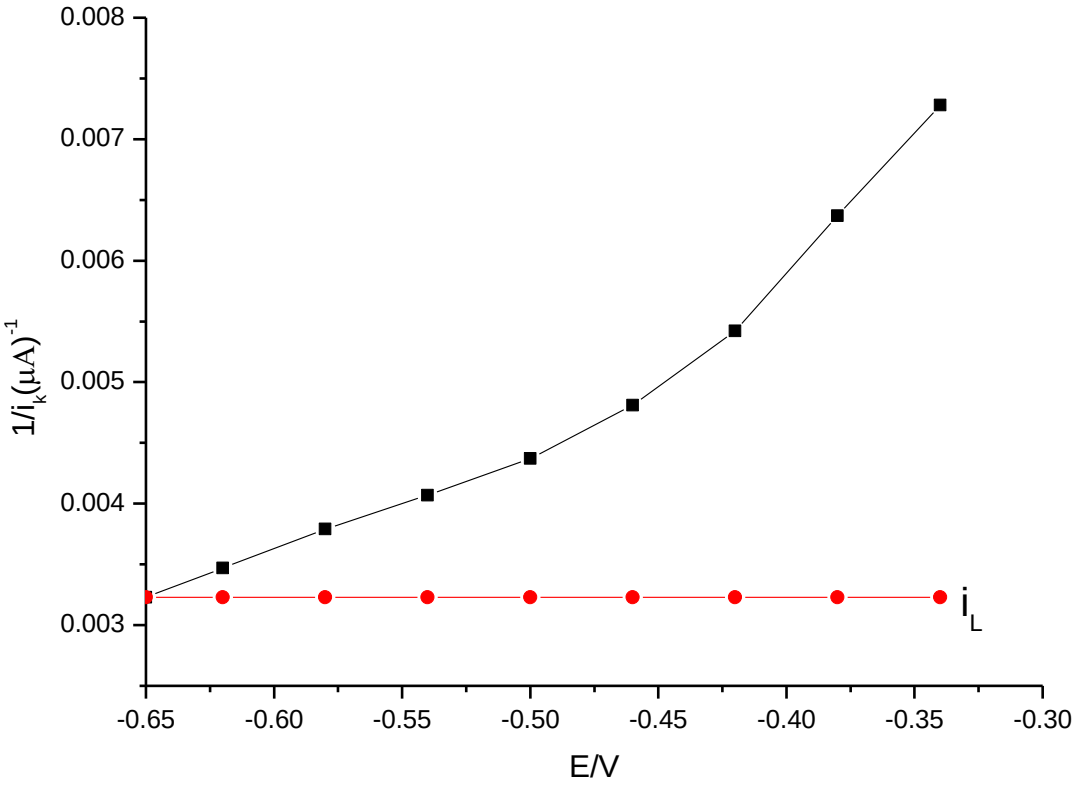

Figure 21. Plot of $1/i_k$ vs electrode potential for reduction of oxygen on GC/MWCNT/DAN in 0.2 M Na_2SO_4 solution (pH=1).

After correction of mass transfer limitation (i_L) in solution, Tafel Plot, $\ln\frac{i}{i_L-i}$ *vs* E (Figure 22) were constructed for analyzing the oxygen reduction kinetics. The plot gives a straight line with a slope 1/b (8.26667) and an intercept at the origin ln (i_L/i^o) (3.0795). From the result a Tafel slope 120 mV/dec and an exchange current of 1.423 x 10^{-5} A were calculated. The value of α for ORR at GC/MWCNT/p-DAN deposited by 5 cycles was calculated using Equation 16 and Tafel slope and found to be 0.217.

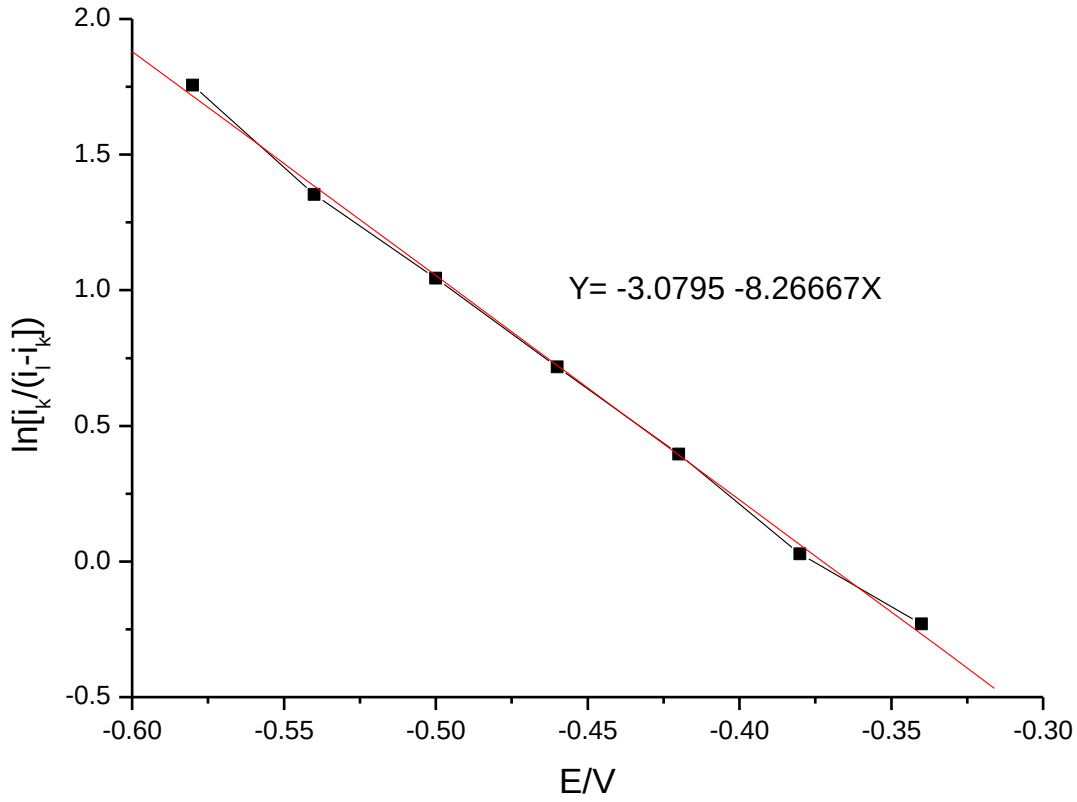

Figure 22. Plot $ln\frac{i_k}{i_L - i_k}$ vs the electrode potential E for reduction of oxygen on GC/MWCNT/DAN electrode in 0.2 M Na_2SO_4 (pH=1) solution.

5.4.2 Oxygen Reduction at MWCNT/p-DAN (8 cycles) Modified GC Electrode

The reduction of oxygen at GC/MWCNT/p-DAN (8 cycles) in oxygen saturated 0.2 M Na_2SO_4 (pH=1) supporting electrolyte was investigated for rotation speed between 100 rpm to 1600 rpm. The current *vs* potential (Figure 23) curves were recorded during slow voltammetric sweep (sweep rate 10 mV/s).

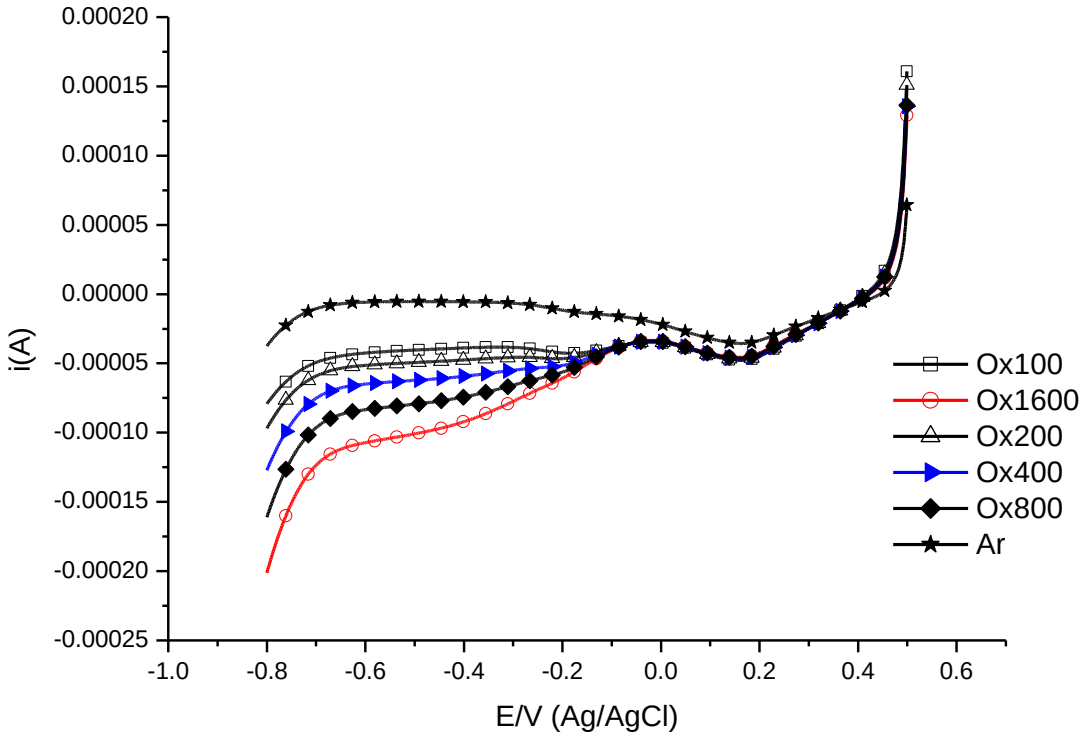

Figure 23. Rotating disc voltammetry curves for oxygen reduction on GC/MWCNT/p-DAN (8 cycles) in O_2-saturated 0.2 M Na_2SO_4 (pH=1) solution in the absence of O_2 (★) and at different rotating rates in the presence of O_2; 100 (□), 200 (△), 400 (▶), 800 (◆), and 1600 (○) rpm.

Figure 24 shows the Levich plot, i_L versus $\omega^{1/2}$ for GC at a potential of -0.6 V. The Levich plot exhibits a good linear (R=0.9996) relationship.

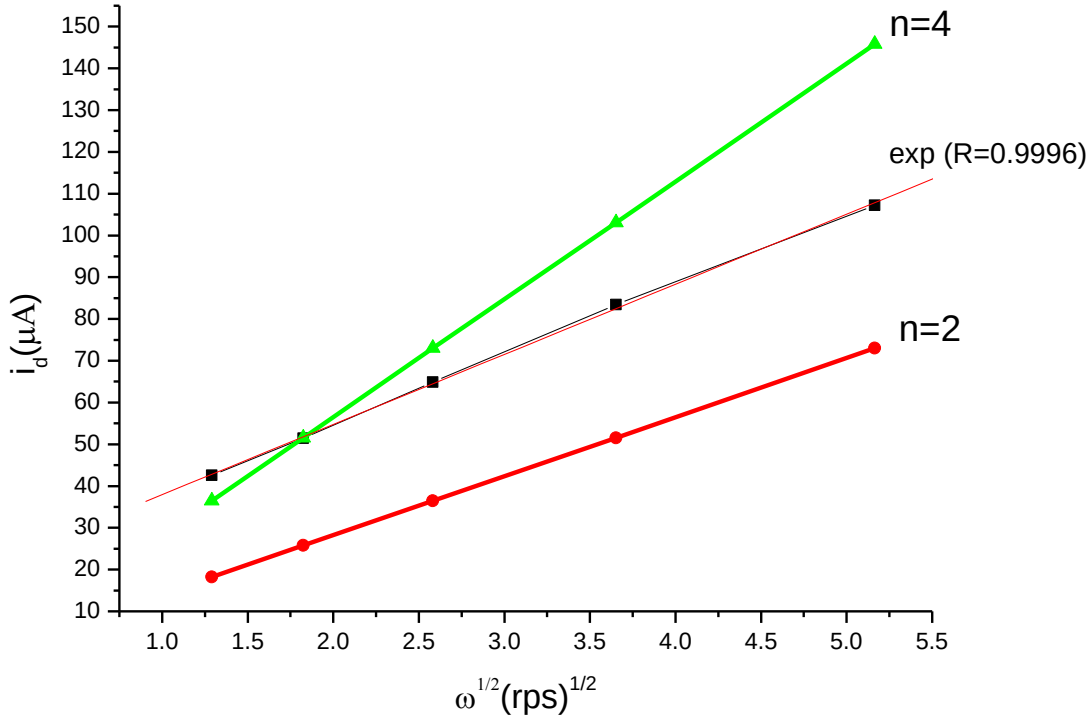

Figure 24. Levich plots for the reduction of oxygen at MWCNT/p-DAN (8 cycles) modified glassy carbon electrode (O_2 saturated 0.2 M Na_2SO_4,10 mV/s) for theoretical (2es and 4es reduction pathways) and experimental result.

The Koutecky-Levich plots corresponding to the experimental values of Figure 23 are shown in Figure 25. From the slope, the number of electrons involved in the reduction of oxygen was found to be 3.88. This suggests that the reduction of oxygen proceeds by the four – electron pathway.

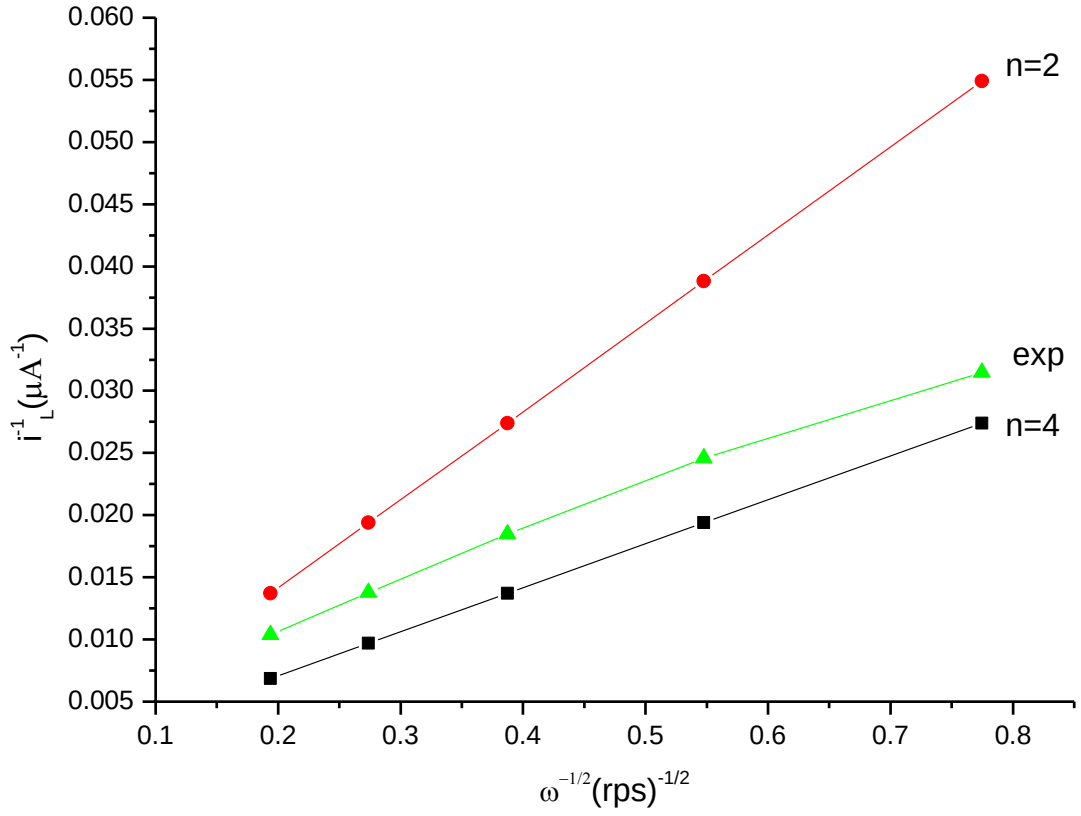

Figure 25. Koutecky –Levich plot of i^{-1} vs $\omega^{-1/2}$for reduction of oxygen on GC/MWCNT/p-DAN (8 cycles) rotating disk electrode for O_2 saturated 0.2 M Na_2SO_4 (pH=1) solution.

The K- L plots at different potential (between -0.3 V to 0.7 V) give straight lines (Figure 26). The slopes remain constant over the potential range. These indicate that a constant numbers of electros are involved in the reduction of oxygen. The intercept of K-L lines at the origin giving the kinetic limiting current (i_k) which are increase as the potential increase to more negative potential.

The rate constant for the reduction of oxygen at GC/MWCNT/p-DAN was determined from K-L plot using Equation 8. From the intercept of the K-L plot (Figure 25) and surface coverage (Γ) from Table 2, the rate constant for the reduction of oxygen was determined to be 1.05×10^3 $M^{-1}s^{-1}$.

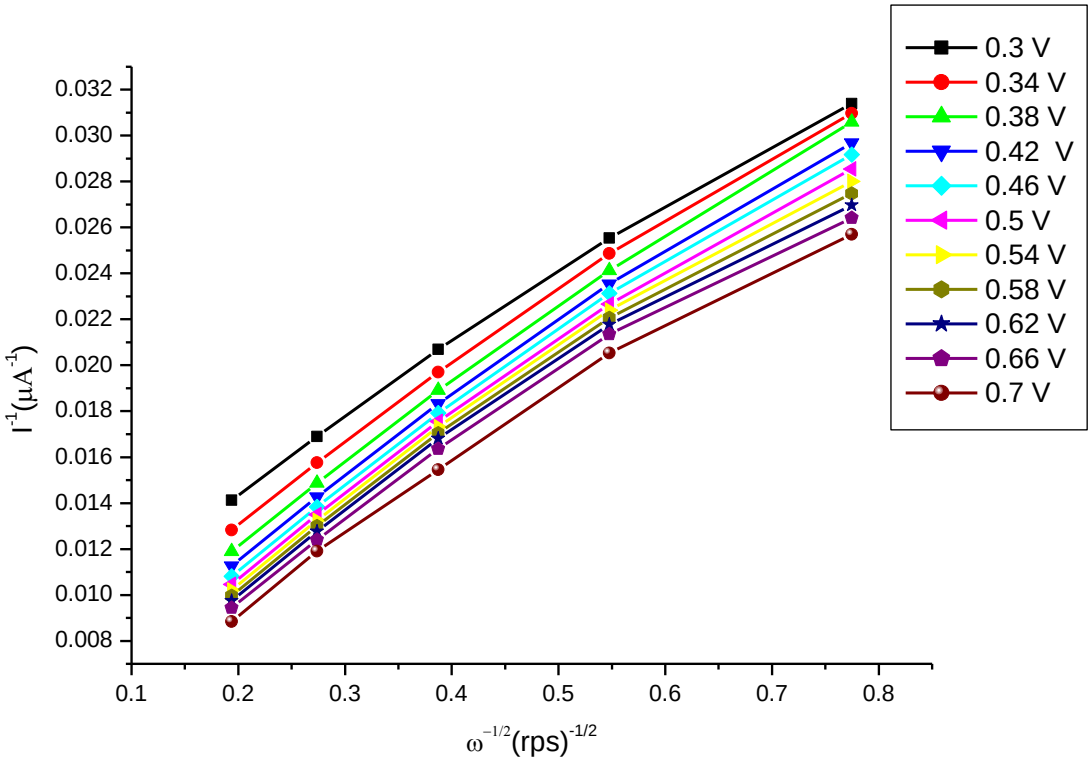

Figure 26. Koutecky- Levich plot for the reduction of oxygen on GC/MWCNT/p-DAN rotating disk electrode in 0.2 M Na_2SO_4 (pH=1) solution at different potential.

Figure 27 shows the plot of 1/ i_k vs the electrode potential (E). These plots allow to determine the limiting current resulting from a mixed control (i_l) obtained by extrapolating Equation (12) at highη. The value of $1/i_l$ obtained was 4640 A^{-1} and limiting current (i_L) for GC/MWCNT/p- DAN (8 cycles) modified electrode was found to be 2.155 x 10^{-4} A.

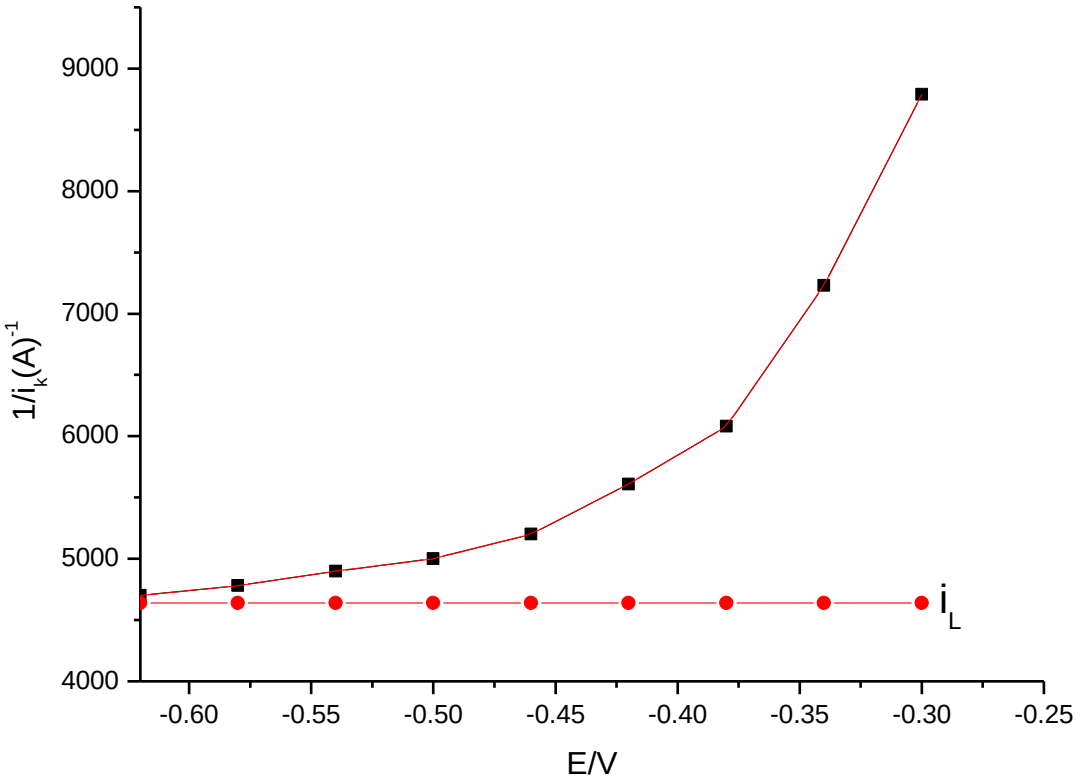

Figure 27. Plot of $1/i_k$ vs electrode potential for reduction of oxygen on GC/MWCNT/p-DAN (8 cycle) in 0.2 M Na_2SO_4 solution (pH=1)

In Figure 28, the mass-transfer corrected Tafel plots ($ln\frac{i_k}{i_L-i_k}$ vs electrode potential) constructed from the RDE data are presented. This plot gives a straight line with a slope 1/b (12.4998) and an intercept at the origin –ln (i_l/i^o) is about -3.56982. From this results Tafel slope 80 mV/dec and an exchange current of 5.366 x 10^{-6} A were calculated. The value of α for ORR at GC/MWCNT/p-DAN deposited by 8 cycles was calculated to be 0.326. The limiting current resulting from a mixed control is higher (about 40 times) than that of the exchange current.

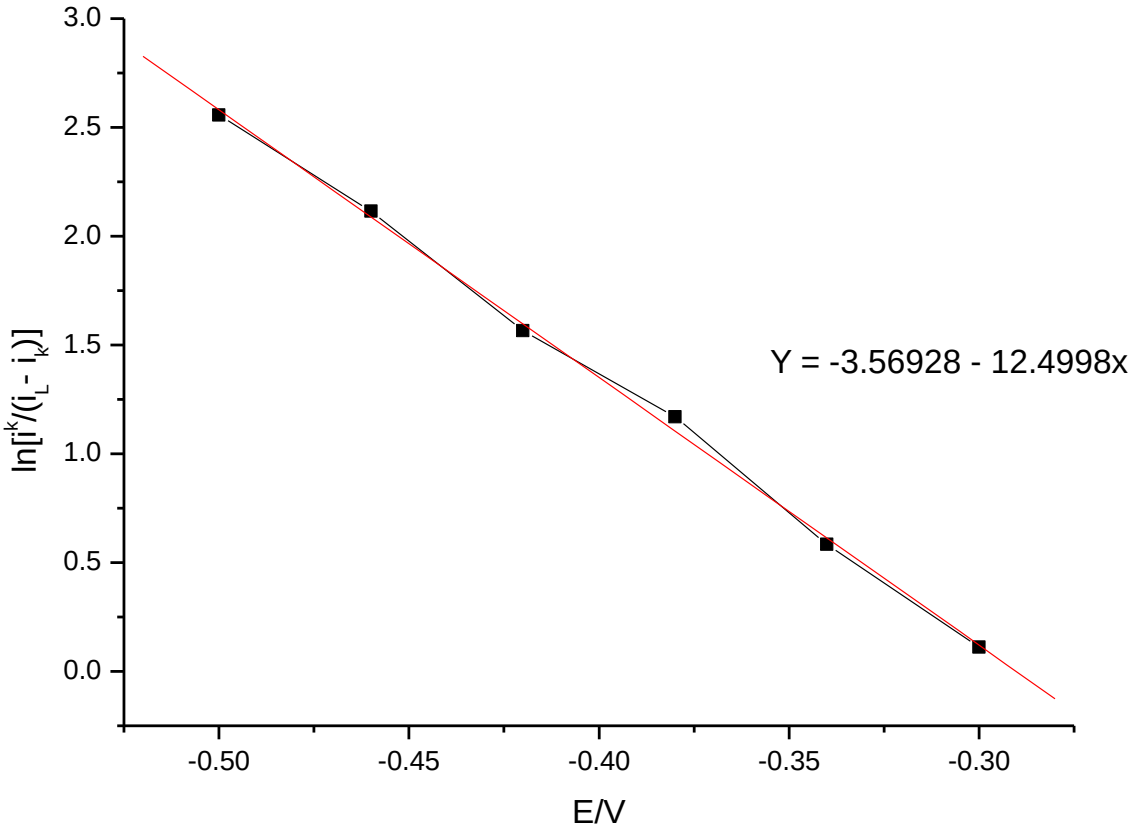

Figure 28. Plot $ln\frac{i_k}{i_L - i_k}$ vs the electrode potential E for reduction of oxygen on GC/MWCNT/p-DAN (8 cycles) electrode in 0.2 M Na_2SO_4 (pH=1) solution.

Table 3 gives the results obtained with GC/MWCNT/p-DAN catalyst at different deposition cycles. It can be observed that ORR mainly occurs via a four electron pathways in studied modified electrodes. The ORR shows better exchange current on GC/MWCNT/p-DAN (5-cycles) than GC/MWCNT/p-DAN (8-cycles) modified electrodes. Therefore, electrode materials or catalyst have better effects on ORR kinetics.

Table 3. The kinetic parameters for the oxygen reduction reaction at GC/MWCNT/p-DAN electrodes at different deposition cycles.

	n	I_L (A)x10^{-4}	I^o (A) x 10^{-5}	k ($M^{-1}s^{-1}$) x 10^3	b (mV/dec)	α
GC/MWCNT/ poly (1, 8- DAN) for 5 cycles	3.7	3.1	1.423	1.499	120	0.217
GC/MWCNT/ poly (1, 8- DAN) for 8 cycles	3.8	2.155	0.536	1.05	80	0.326

6. Conclusions

In this study we have demonstrated the presence of a specific interaction of carbon nanotubes with poly (1, 8- DAN) and polypyrrole resulting in a very good enhancement of the electrochemical properties of the polymers.

The MWCNT/ poly (1, 8- DAN) and MWCNT/ polypyrrole were used to prepare modified GC electrode for reduction of oxygen in oxygen saturated 0.1 M Na_2SO_4 (pH= 1) solution. The result obtained show a favorable potential shift of about 190 mV and six fold increase in the current at the GC/MWCNT/ poly (1, 8- DAN) electrode compared to the value obtained at GC/MWCNT electrode.

Based on the RDV experimental results, the numbers of electrons transfer of O_2 reduction, (n) limiting current (i_L), exchange current (i^0), heterogeneous rate constant of ORR (k), Tafel slopes(b), and transfer coefficient (α) of GC/MWCNT/ poly (1, 8- DAN) at different deposition cycles were calculated and summarized in Table 3.

References

1. L. Genies, R. Faure, R. Durand, *Electrochim. Acta*, 44 (1998), 1317 - 1327.

2. Y. F. Yang, Y.H. Zhoij and C.S. Chat, *Electrochim. Acta*, 40 (1995) 2579 - 2586.

3. V.D. Noto, E. Negro, *Electrochim. Acta*, 55 (2010) 1407 - 1418.

4. J. M. Ziegelbauer, V. S. Murthi, C. O'Laoire, A. F. Gull, S. Mukerjee, *Electrochim. Acta*, 53 (2008) 5587 - 5596.

5. R. Sulub S., W. M. Millan, M. A. Smit, *Int. J. Electrochem. Sci*., 4 **(**2009**)** 1015 – 1027.

6. L. Agui, P. Y. Sedeno, J. M. Pingarron, *Anal. Chimica Acta*, 622 (2008) 11 – 47.

7. J. Lipkowski and P.N. Ross, Electrocatalysis, Wiley-VCH, New York, (1998), 1997 - 213.

8. R. R. Adzic and J. X. Wang, *J. Phys. Chem. B*, 102 (1998), 8988 - 8993.

9. J. X. Wang, F. A. Uribe, T. E. Springer, J. Zhang and R. R. Adzic, *Faraday Discuss.*, 140 (2008) 347 - 362.

10. C. V. A. Rao, *Ph. D. Dissertation*, India Institute of Technology Madras, India, 2008, 7-20.

11. M. C. Pelsozy, *Ph. D. Dissertation*, Case Western University, Ohio, 2008, 9 - 12.

12. J. Kim and A. A. Gewirth, *Bull. Korean Chem. Soc*., 28 (2007**)** 1322 - 1328

13. E. D. Jeong. M. S. Won and Y. B. Shim, *Bull. Korean Chem. Soc*,. 19 (1998) 417 - 422.

14. S. Swavey, M. Narra, and H. Srour, *J. Coord. Chem.,* 58 (2005), 16, 1463 - 1476.

15. J. N. Coleman, U. Khan, W. J. Blau, Y. K. Gunko, *Carbon*, 44 (2006) 1624 - 1652.

16. R. Khare and S. Bose, *J.Mina. and Materi. Chara.& Engi.*,14 (2005) 1, 31 - 46.

17. E. G. Rakov, *Russian Chemical Reviews*, 70 (2001) 10, 827 – 863.

18. K. Balasubramanian and M. Burghard, *Small*, 1 (2005) 2, 180 - 192.

19. T. Byrne and Y. K. Gunko, *Adv. Mater.*, 27 (2009) 1 - 17.

20. J.W. Seo, E. Couteau, P. Umek, K. Hernadi, P. Marcoux, B. Lukic, C. Miko, M. Milas, R. Gaal and L.Forro, *New J. of Phys.*, 5 (2003) 120, 120–143.

21. U. Lange, N. V. Roznyatovskay, V. M. Mirsky, *Anal. Chimica Acta*, 614 (2008) 1–26.

22. J. N. Coleman, U. Khan, W. J. Blau, Y. K. Gunko, *Carbon*, 44 (2006) 1624 - 1652.

23. X. R. Ye, Y. Lin, C. Wang, M. H. Engelhard, Y. Wanga and C. M. Wai, *J. Mater. Chem*, 14 (2004) 908 – 913.

24. C. Peng, S. Zhang, D. Jewell, G. Z. Chen, *Progress in Natural Science*, 18 (2008) 777 – 788.

25. M. Wu, L. Zhang, D. Wang, J. Gao and S. Zhang, *Nanotechnology*, 18 (2007) 385, 603 - 611.

26. K. M. Manesh, P. Santhosh, A. I. Gopalan, and K. P. Lee, *Electroanalysis*, 18 (2006) 16, 1564 – 1571.

27. P. Santhosh, K. M. Manesh, K. P. Lee and A. I. Gopalan, *Electroanalysis*, 18 (2006) 9, 894 – 903.

28. U. Yogeswaran and S. M. Chen, Anal. Letters, 41 (2008) 210 – 243.

29. M. Moniruzzaman and K. I. Winey, *Macromolecules*, 39 (2006) 5194 - 5205.

30. G.G.Wildgoose, C.E. Banks, R.G. Compton, *Small*, 2 (2006) 182 - 193.

31. G.W. Yang, G.Y. Gao, C. Wang, C.L. Xu, H.L. Li, *Carbon*, 46 (2008) 747 – 752.

32. Y. Shi, R. Yang, P. K. Yueta, *Carbon*, 47 (2009) 1146 – 1151.

33. C.T. Hsieh, J. Y. Lin, J. L. Wei, *Inter.J. of Hydrogen Energy*, 34 (2009) 685 - 693.

34. N. Alexeyeva, K. Tammeveski, *Anal. Chimica Acta*, 618 (2008) 140–146.

35**.** N. Alexeyeva, L. Matisen, A. Saar, P. Laaksonen, K. Kontturi, K.Tammeveski, *J. Electroanal. Chem.*, 642 (2010), 6 - 12

36. J. Qu, Shen, X. Y. Qu, S. Dong, *Electroanalysis*, 16 (2004) 17, 1444 - 1450.

37. K. M. Manesh, P. Santhosh, A. I. Gopalan, K.P. Leea, *Electroanalysis*, 18, (2006**)** 16, 1564 – 1571.

38. N. Alexeyeva, K. Tammeveski, *Anal. Chimica Acta*, 618 (2008) 140–146.

39. A..J. Bard, and L.R. Faulkner, Electrochemical Methods: Fundamentals and *Applications*, 2nd ed., John Wiley and sons, New York, 2000.

40. J. Wang, *Analytical electrochemistry*, 3rd ed., John Wiley and sons, New York, 2006.

41. S. Treimer, A. Tanga, and D. C. Johnson, *Electroanalysis*, 14 (2002), 3, 165-171.

42. M. Gojo, V. D. Stankovi and S. M. Poljacek, *Acta. Chim. Slov.*, 55 (2008) 330–337.

43. G. Pandi, S. Ramiah, *J. Phys. Chem. C,* 111 (2007) 30, 11320-11328.

44. H. Park, T. Kwon, D. S. Park and Y. B. Shim, *Bull. Korean Chem. Soc,*.27 (2006) 1763-1768.

45. G. Han, J. Yuan, G. Shi, F. Wei, *Thin Solid Films,* 474 (2005) 64-69.

46. C. Coutanceau, M. J. Croissant, T. Napporn, C. Lamy, *Electrochim. Acta,* 46 (2000) 579-588.

47. L. Demarcony, C. Coutanceau, J. M. Leger, *Electrochim. Acta,* 53 (2008) 3232-3241.

48. M. Pattabi, R.H. Castellanos, R. Castillo, A.L. Ocampo, J. Moreira, P.J. Sebastian, J.C. McClure, X. Mathew. *Inter.J. of Hydrogen Energy,* 26 (2001) 171 - 174.

49. S. Y. Honga, S. M. Parkb, *J. Electro. Soc.,* 150 (2003) 7, 360 - 365.

50. P.A. Mabrouk, *Synthetic Metals,* 150 (2005) 101 - 105.

51. C. M. A. Brett and A. M. O. Brett, *Electrochemistry: Principles, Methods, and Applications,* Oxford University Press Inc., New York, 1994.